WestVirginiaUniversity
THE RESEARCH REPOSITORY @ WVU

Graduate Theses, Dissertations, and Problem Reports

2023

Accelerating Manufacturing Decisions using Bayesian Optimization: An Optimization and Prediction Perspective

Taofeeq Olajire
West Virginia University, too00002@mix.wvu.edu

Follow this and additional works at: https://researchrepository.wvu.edu/etd

 Part of the Industrial Engineering Commons, Manufacturing Commons, Other Operations Research, Systems Engineering and Industrial Engineering Commons, and the Systems Engineering Commons

Recommended Citation

Olajire, Taofeeq, "Accelerating Manufacturing Decisions using Bayesian Optimization: An Optimization and Prediction Perspective" (2023). *Graduate Theses, Dissertations, and Problem Reports*. 12076.
https://researchrepository.wvu.edu/etd/12076

This Thesis is protected by copyright and/or related rights. It has been brought to you by the The Research Repository @ WVU with permission from the rights-holder(s). You are free to use this Thesis in any way that is permitted by the copyright and related rights legislation that applies to your use. For other uses you must obtain permission from the rights-holder(s) directly, unless additional rights are indicated by a Creative Commons license in the record and/ or on the work itself. This Thesis has been accepted for inclusion in WVU Graduate Theses, Dissertations, and Problem Reports collection by an authorized administrator of The Research Repository @ WVU. For more information, please contact researchrepository@mail.wvu.edu.

Accelerating Manufacturing Decisions using Bayesian Optimization: An Optimization and Prediction Perspective

Taofeeq Olajire

A thesis submitted to the

College of Engineering and Mineral Resources at

West Virginia University

Master of Science in Industrial Engineering

Imtiaz Ahmed, Ph.D., Chair

Zhichao Liu, Ph.D.

Omar Al-Shebeeb, Ph.D.

Department of Industrial and Management Systems Engineering

Morgantown, West Virginia

July 2023

Keywords: Multi-objective optimization, Bayesian Optimization, Additive Manufacturing, Epsilon-greedy Methods, Gaussian Process

Copyright 2023 Taofeeq Olajire

Abstract

Accelerating Manufacturing Decisions using Bayesian Optimization: An Optimization and Prediction Perspective

Taofeeq Olajire

Manufacturing is a promising technique for producing complex and custom-made parts with a high degree of precision. It can also provide us with desired materials and products with specified properties. To achieve that, it is crucial to find out the optimum point of process parameters that have a significant impact on the properties and quality of the final product. Unfortunately, optimizing these parameters can be challenging due to the complex and nonlinear nature of the underlying process, which becomes more complicated when there are conflicting objectives, sometimes with multiple goals. Furthermore, experiments are usually costly, time-consuming, and require expensive materials, man, and machine hours. So, each experiment is valuable and it's critical to determine the optimal experiment location to gain the most comprehensive understanding of the process. Sequential learning is a promising approach to actively learn from the ongoing experiments, iteratively update the underlying optimization routine, and adapt the data collection process on the go. This thesis presents a multi-objective Bayesian optimization framework to find out the optimum processing conditions for a manufacturing setup. It uses an acquisition function to collect data points sequentially and iteratively update its understanding of the underlying design space utilizing a Gaussian Process-based surrogate model.

In manufacturing processes, the focus is often on obtaining a rough understanding of the design space using minimal experimentation, rather than finding the optimal parameters. This falls under the category of "approximating the underlying function" rather than design optimization. This approach can provide material scientists or manufacturing engineers with a comprehensive view of the entire design space, increasing the likelihood of making discoveries or making robust decisions. However, a precise and reliable prediction model is necessary for a good approximation. To meet this requirement, this thesis proposes an epsilon-greedy sequential prediction framework that is distinct from the optimization framework. The data acquisition strategy has been refined to balance exploration and exploitation, and a threshold has been established to determine when to switch between the two. The performance of this proposed optimization and prediction framework is evaluated using real-life datasets against the traditional design of experiments. The proposed frameworks have generated effective optimization and prediction results using fewer experiments.

ACKNOWLEDGEMENT

I am profoundly grateful to God for his mercy over me, and to my advisor, Dr. Imtiaz, and the committee for their inestimable guidance, expertise, and unstinting support throughout the entire process of completing this thesis. Their wisdom, patience, and insightful feedback have been essential in shaping the direction of my research and refining my ideas. I am truly indebted to them for their dedication and mentorship.

I would also like to express my sincere appreciation to Tobi Ore and Hamed Khosravi for their contributions to various aspects of this research. Their collaboration and willingness to offer their expertise have been invaluable in broadening the scope and quality of this work.

Finally, I wish to express my heartfelt gratitude to my family and friends for their unconditional love, support, and encouragement throughout this endeavor. Their belief in me and constant encouragement have been the driving force behind my achievements.

To all those who have played a role, great or small, in the completion of this thesis, I offer my most sincere thanks. Your support, encouragement, and guidance have made a significant difference in my academic journey, and I am truly grateful for your presence in my life.

TABLE OF CONTENTS

LIST OF FIGURES

LIST OF TABLES

LIST OF ABBREVIATION

3DP	3D printing
AI	Artificial Inteligence
AM	Additive mnaufacturing
BO	Bayesian optimization
BJ	Binder jetting
CAD	Computer-aided design
CAM	Computer-aided manufacturing
CNC	Computer numerical control
DACE	Design and analysis of computer experiment
DED	Direct energy deposition
DOE	Design of experiment
EGO	Efficient global optimization
FDM	Fused deposition modeling
FFF	Fused filament fabrication
G_exp	Shear modulus
GP	Gaussian process
ICT	Information and communication technology
IOT	Internet of things
K_exp	Bulk modulus
LBAM	Laser-based additive manufacturing
LHS	Latin hypercube sampling
M-APO	Multi-objective accelerated process optimization
MDS	Material design space
ML	Machine learning
MOBO	Multiobjective Bayesian optimization
MOGA	Multi-objective genetic algorithm
NN	Neural network
MOO	Multiobjective optimization
PHV	Proportional hypervolume
qParеGo	Parallel efficient global optimization
RMSE	Root mean square error
SLA	Stereolithography
SLS	Selective laser sintering
STL	Standard triangle language
UTS	Ultimate tensile strength

1. Introduction

Information and communication technology (ICT) plays a crucial role in the realm of manufacturing systems. The continuous development of cyber systems and associated intelligent and smart technologies has resulted in the emergence of significant concepts such as big data [1], Industry 4.0, the Internet of Things (IoT), cloud computing, cyber-physical systems (CPSs), digital twin (DT), and next-generation artificial intelligence (AI) [2]. Industry 4.0 is primarily based on intelligent manufacturing system paradigms, including flexible manufacturing and reconfigurable manufacturing [3].

The utilization of Artificial Intelligence (AI), particularly machine learning (ML), is increasingly becoming prevalent in factory operations. Previous studies have extensively examined the application of machine learning, data mining, and other AI techniques in various years. For instance, Harding et al. [4] provided an overview of AI applications spanning from 1987 to 2005. Additionally, recent years have witnessed the adoption of advanced statistical techniques like machine learning to predict part quality characteristics.

The trend of AI, specifically ML, remains strong and is further amplified by the growing emphasis on digitalization. While machine learning is a subset of AI, its practical implementation in industrial settings has gained momentum only recently, as demonstrated in this article. The ongoing process of digitalization in the industry is accompanied by an exponential increase in data, leading to larger datasets that can be utilized by ML applications to extract knowledge from historical events.

The optimization of control parameters is often necessary for physical experiments to achieve optimal outcomes, resulting in a growing interest in the utilization of machine learning algorithms in this field. The nature of optimization problems can be categorized as either single-objective or multi-objective, depending on the number of objective functions to be minimized or maximized. Although single-objective optimization methods have been widely adopted in manufacturing, there is already a notable research focus on multi-objective optimization (MOO) to facilitate the development of high-quality and cost-effective products across various branches of manufacturing engineering.

In any manufacturing process, a difficult task is to balance the resultant properties. For example, a particular process may result in high yield strength, but it may cause lower ductility or elongation to failure, while low cooling rates may result in high surface roughness. Because of the conflict among a variety of mechanical properties, it is extremely difficult to identify the optimal process/design parameters for fabricating parts that maintain an acceptable level of various mechanical properties at the same time. Consequently, the optimization of the process concerning various mechanical properties should be considered a multi-objective process.

By using sample-efficient Bayesian optimization (BO) [48], manufacturing processes can be optimized for difficult-to-measure, black-box performance measurements. The Bayesian optimization process (BO) involves adjusting design parameters to optimize black-box performance measures that are difficult to evaluate in manufacturing processes. In several manufacturing processes, design parameters are susceptible to random energy losses, which may result in a product that performs less well than expected. Nevertheless, the BO method has been presented for optimizing a single technology. There is no existing technique capable of dealing with real-world situations in which multiple goals are sensitive to input fluctuations. In scientific and engineering fields, optimization problems are commonly encountered as a means of modifying several parameters. Numerous black-box objective functions conflict with one another. Most often, a single design does not meet all the objectives in the best way.

Therefore, the purpose of multi-objective optimization (MOO) is to locate the Pareto frontier (PF) of the best trade-offs. PF helps to identify the set of Pareto-efficient solutions and to choose among them instead of considering the full range of solutions. There is a connection between the objectives and the appropriate designs that accompany them. Multi-objective optimization methods are categorized into two main categories: scalarization or aggregation methods and evolutionary algorithms [5]. Typically, scalarization methods convert multi-objective optimization problems into single-objective optimization problems and then solve them using routine single-objective optimization problem solvers [6]. Due to the lack of a functional representation of the relationship between process variables and mechanical properties, this class of methods does not apply to multi-objective optimization required in manufacturing processes.

In many cases, it is necessary to measure the objectives through resource-intensive modeling or testing. Therefore, any method useful for optimizing these functions must be significantly sample-efficient; in other words, it must identify the optimal parameters for the goal functions by simply examining a limited number of designs. Shahriari et al. [7], recommend Bayesian optimization (BO) as a method for resolving this class of problems.

Another challenge that arises in the manufacturing decision-making landscape is approximating the underlying design space or function. This involves modeling the relationship between the input variables, such as process conditions, and the output variables, such as performance or quality. The goal is to make accurate predictions of output values for future processing conditions. This is distinct from finding the optimal process conditions where the algorithm only looks for maximum and minimum points and ignores other defining relationships.

In prediction, it is crucial to understand all regions of the design space instead of focusing solely on high-return areas. This creates a dilemma known as the "exploration vs exploitation" problem in data mining. Exploitation involves follow-up investigations of current patterns or findings by conducting experiments in a nearby region, while exploration entails conducting experiments in different regions to search for new clues, avoiding getting stuck in local optima. Exploitation can help reach the most rewarding points faster, making it better for optimization, while exploration can help escape a particular region and approximate different parts of the design space more quickly, making it better for prediction. A balance between exploration and exploitation is essential for promoting an effective optimization and prediction framework.

In the BO framework, an acquisition function usually dictates the algorithm to choose the next experiment location, i.e., where to conduct the next experiment. The current acquisition functions utilized in the optimization framework prioritize exploitation, which is not optimal for prediction. To address this, the acquisition function needs to be modified to incorporate more exploration. One approach could be setting a pre-determined threshold that determines when to switch between exploration and exploitation. At each iteration, a random number can be generated and compared to the threshold to decide between exploration or exploitation.

In Figure 1, an illustration of a candidate manufacturing process is provided. It is known as Direct energy deposition (DED) which is an additive manufacturing (AM) process. In AM, three-dimensional (3D) models are produced by depositing material layer by layer [9]. In general, it refers to the process of fabricating 3D objects directly from CAD models in a layer-by-layer manner. Three stages are involved in the AM process: the pre-printing, the printing, and the post-processing steps.

Although DED has many advantages, its complicated thermal history still poses significant barriers to its widespread application in terms of quality, surface finish, and repeatability. It has many controllable parameters that are reported to impact the adhesive powder deposition procedure and subsequent solidification heat transfer during fabrication. Accordingly, the quality of the final part's microstructure and mechanical properties is strongly affected by the parameters of the production process [12]. Numerous cases have been reported in which the relationship between various mechanical properties (or geometric characteristics) of the fabricated parts appears to be contradictory which calls for a multi-objective optimization approach. Furthermore, the DED experiments are costly and the optimization approach needs to identify the Pareto frontier in a sample-efficient way. Similar to DED, other AM processes and traditional machining processes also face these problems of property optimization and understanding the process-property relationship in fewer manufacturing runs.

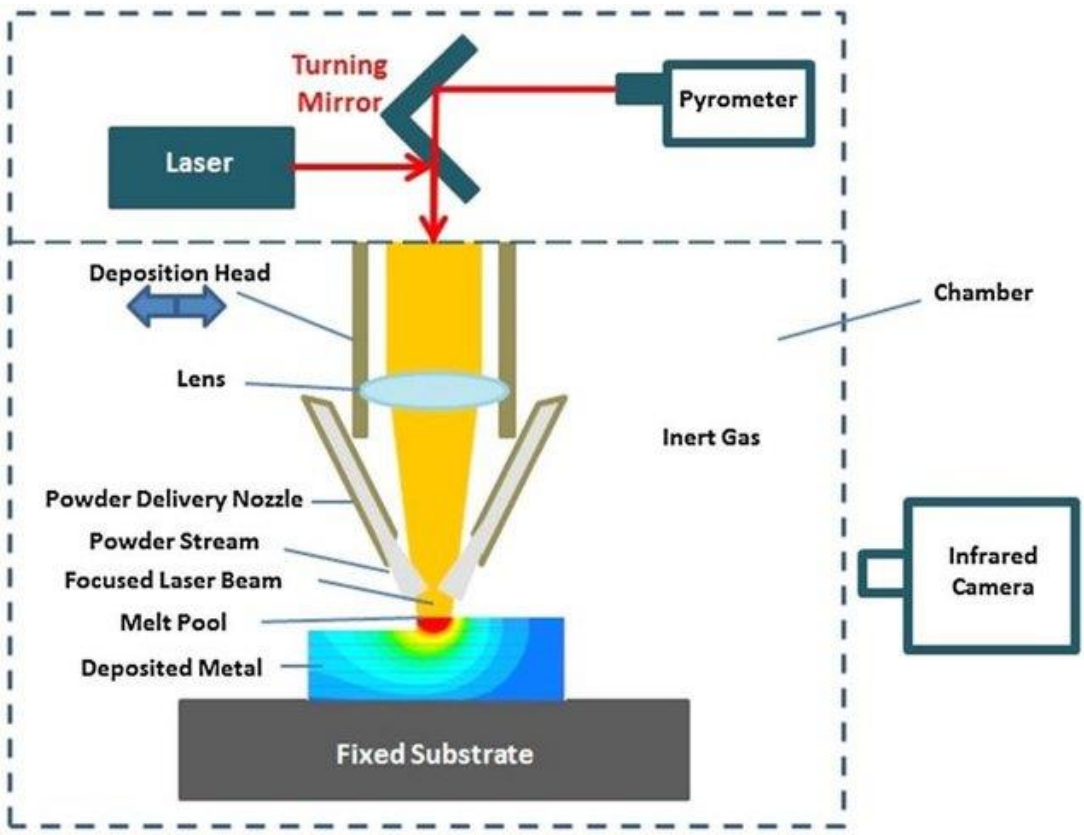

Figure 1: Illustration of the DED process [13]

Considering the above discussion, the objectives of this research are thus given below:

a) To develop a multi-objective Bayesian Optimization framework to find out the optimum processing conditions in a manufacturing set up.
b) To develop an epsilon-greedy sequential prediction framework to effectively approximate the underlying manufacturing design space.
c) To illustrate the performance of both frameworks by replicating an active learning scenario using several real-life datasets.

The rest of the report has been divided into sections as follows. Chapter 2 highlights the literature review based on research works related to prediction and optimization in AM. It also presents a detailed bibliometric analysis. In Chapter 3, the methodologies considered for this work are described. The characteristics of the datasets utilized are described in Chapter 4. The comparative

performance of the proposed approaches is detailed in Chapter 5. Finally, this thesis is concluded in Chapter 6.

2. LITERATURE REVIEW

A unique optimization and prediction method for manufacturing has been developed in this research that anticipates and optimizes process parameters. An analysis of the literature on prediction and optimization in manufacturing technologies is presented in this chapter to identify knowledge gaps that have not been addressed by previous research. Firstly, a review of the prediction model in manufacturing is discussed, followed by a review of publications on optimization in manufacturing. Finally, a bibliometric analysis of the literature is presented. Due to the current advancements and popularity of AM technologies, the focus of this review is primarily on AM-related research works.

2.1. Research Work on Prediction

Machine learning prediction has attracted substantial interest in the manufacturing sector due to its capacity to increase prediction accuracy and dependability. This has led to increased production efficiency and cost savings. The goal of this sub-section is to look at current developments in machine learning prediction models and how they are used in the manufacturing sector.

In 1999, Luo et al. [14] measured the power density of three types of additive manufacturing processes, namely fused deposition modeling (FDM), selective laser sintering (SLS), and stereolithography (SLA). Similarly, Srinivasan and Burell [15] used a similar methodology to estimate the average energy consumption per process performance of SLS technology. A similar technique was employed by Watson and Taminger [16] to model the typical energy consumption per unit volume of material in 2018. The simple volumetric modeling approach can provide a quick estimate of energy consumption, but it does not account for variations in G-code or power consumption when the same amount of material is processed with different settings or on different AM machines. Therefore, it is necessary to develop a more comprehensive predictive model that incorporates mechanical properties as well as process parameters. In 2014, Meteyer et al. [17] developed a simulation method to predict the energy consumption of a binder jetting (BJ) process at the unit level. As part of the proposed method, the binder jetting machine (BJ) was broken down

into its energy-intensive components, which included curing ovens, infrared heaters, rollers, print heads, and sintered parts. The power consumption and duration of each component were measured in an experiment. Nevertheless, the simulation method can only be applied to BJ technology and cannot be extended to other AM processes.

The energy consumption of three FDM machines was assessed under different operating conditions, such as start-up, warm-up, preparation, and assembly. To estimate the energy consumption of FDM machines, a consumption model was developed by measuring the power requirements for each operational state and determining the time required to deposit material by Peng and Sun [18]. Data collected from the AM machine, such as component temperatures, running time, and power consumption, was collected in real time. Using data analysis techniques, the data was analyzed and characterized, and the information was uploaded to a cloud database based on process parameters and design specifications.

The cloud has been aggregated with all the necessary information to retrieve power consumption information for AM machines, including details on power consumption status, behavior, and forecasts. Even though no specific algorithms or methods for data analysis have been developed yet, the framework outlines a basic workflow for energy estimation. In 2018, Qin et al. [19] proposed a data-driven modeling method utilizing clustering and deep learning techniques to estimate energy consumption.

The melt pool is a key component of process monitoring for additive manufacturing operations such as powder bed fusion (PBF), where most monitoring investigations are conducted. Using melt pool thermal data, Kwon et al. [20] developed a CNN-based software that distinguishes between high and low-quality constructions with a failure rate of less than 1.1%, potentially saving time and money. According to Zhang et al. [21], integrating melt pool, plume, and spatter data produces the best results for categorizing component quality. Long-short-term memory networks (LSTMs) have been shown to provide better predictions than other neural networks (Zhang et al. [22]).

Using 30 training data, Caiazzo et al. [23] were able to predict trace geometry using BP-NN with an average RMSE of approximately 5%. According to Rong-Ji et al. [24], they evaluated the performance of BP-NN with varying numbers of hidden neurons and concluded that more hidden

neurons tend to result in better predictions. Using recurrent neural networks in the ME process, Zhang et al. [13] predicted the tensile strength of printed products with an RMSE of approximately 2%. In this application, a recurrent neural network outperformed a random forest and a support vector regression algorithm. While NNs demonstrated excellent performance in regression tasks, multiple hyperparameters such as the number of hidden neurons and layers needed to be tuned. The use of an ensemble of multiple algorithms, including neural networks, has also been reported [25], which has been found to perform better than neural networks alone and can be considered as an alternative to neural networks. According to Aoyagi et al. [26], EBM flowcharts can be created from only eleven datasets using a simple approach. This study used SVM solely for fitting the data and identifying decision boundaries. As a result of the small size of the training dataset, evaluating the model's accuracy was challenging. For the prediction of time series, RNNs are commonly used. Using RNNs to train FEM data, Mozaffar et al. [27] determined the high thermal history of complex DED components. Additionally, both MLP and SVM have been applied to the prediction of thin wall deposits in DED.

Further, Z. Li et al. [28] predicted surface roughness in laser additive manufacturing using RF, AdaBoost, RT, SVR, Ridge regression, and NN models. A total of 108 input features were used in this study, including extruder temperature, printing speed, and layer thickness. Francis et al. [29] developed a CNN-based machine learning model for geometric error compensation in L-PBF. Using thermal history and processing parameters as inputs, the model predicts distortion and reverse-imports it to the CAD model to compensate for errors.

In their study of 3D response maps to melt pool depths vs. process settings, Tapia et al. [30] utilized a Gaussian Process-based (GP) substitute model. In this way, parametric combinations could be defined to prevent keyhole melting. To obtain 139 valid data points, one empirical dataset and two literature datasets were combined, and several filters were applied in order to reduce abnormalities. Despite their 6.023 μm preview error, machine learning can be used to study the macroscale characteristics of AM-built objects in addition to verifying the operating parameters. Using 139 SS316 L fatigue data manufactured under 18 different treatment configurations on the same SLM equipment, Zhang et al. [31] developed a fuzzy inference system based on adaptive systems (ANFIS). Although their algorithms had an average root squared error of 11-16%, the use of the training set with 66 data points resulted in a reduction in performance due to the variability of the

mechanical system from one machine to another. When training models, it is recommended to use both empirical and bibliographical inputs to increase the likelihood of generalization. Material extrusion has used optical tracking to detect defects in real time. A classification method was used by Wu et al. [32] for detecting infill print faults in material extrusion with a 95% accuracy rate, without considering other quality metrics such as precision and recall.

After going through the literature review, it is evident that even though there has been a lot of work and publication on prediction methodology using machine learning, however, it has never been used simultaneously with sequential optimization.

Table 1: A Summary of Prior Studies on Prediction in the Manufacturing Industry

Ref.	**Year**	**Prediction method used**	**Focus**
(Luo et al., 1999)	1999	Volumetric modeling approach	Measured SLS, FDM and SLA
(Rong-Ji et al., 2009)	2009	Neural Network	Evaluated the performance of BP-NN
(Meteyer et al., 2014)	2014	Simulation method	Used simulation method to predict binder jetting methods
(WU et al., 2016)	2016	Classification method	Using classification to detect infill print faults in material extrusion
(Peng and Sun, 2017)	2017	Consumption method	Estimating the energy consumption in FDM
(Tapia et al., 2017)	2017	Gaussian process based	3D response map for melt pool with process settings
(Watson and Taminger 2018)	2018	Fuzzy rule-based system	Energy consumption, tooling costs, and productivity

Ref.	Year	Prediction method used	Focus
(Qin et al., 2018)	2018	Clustering and deep learning	Estimating energy consumption
(Mozaffar et al., 2018)	2018	Recurrent neural network	Determine the high thermal history in DED
(Zhang et al.,2019)	2019	Fuzzy inference system	Predicting fatigue in SLM
(Francis et al., 2019)	2019	Convolutional neural network	To achieve the geometric error compensation in laser power bed fusion
(Aoyagi et al., 2019)	2019	Support vector machine	Used small dataset for prediction
(Zhang et al., 2020)	2020	Long-short-term-memory networks	Categorizing component quality

2.2. Research Works on Optimization

Optimization in manufacturing has emerged as a crucial topic of research due to the demand for greater productivity and efficiency in the competitive global market. The goal of this subsection is to examine the most recent state-of-the-art strategies and techniques for manufacturing process optimization.

Amir et al., [33] investigated the measurement of geometry accuracy in parts manufactured using the Fused Filament Fabrication (FFF) process. A novel bi-objective process optimization framework based on the scalarization concept was presented, which solved a series of single-objective sub-problems to achieve optimal properties more efficiently than existing methods. In

another article [34], Amir et al. focused on optimizing mechanical properties by optimizing the process of Laser-Based Additive Manufacturing (LBAM). To account for the effects of voids' size and distribution on the mechanical properties of the final part, the researchers used the multi-objective accelerated process optimization (m-APO) method. The m-APO approach decomposed the multi-objective optimization problem into a series of single-objective subproblems that maximized the relative density and elongation-to-failure of parts fabricated using selective laser melting (SLM). M-APO helped to achieve optimal process parameter settings while reducing the time and cost of experiments by 51.8% compared to the extended full factorial design plan.

Hertlein et al. [35] investigated unit cell design optimization, which involves optimizing height, width, and strut thickness, and lattice structure design optimization, which involves two additional design variables: the number of rows and columns of unit cells. For both optimization problems, the objective function was a weighted sum of the head injury criterion and the part volume. There are two types of unit cells (diamond and honeycomb) that are defined by geometric attributes such as height, width, and strut thickness. Since nonlinear finite element analysis is computationally expensive and obtaining objective gradient information is challenging, the authors employed a Gaussian process (GP) model to approximate the objective function. In the unit cell design optimization, the GP model was initialized with four random training points, whereas in the lattice structure design optimization, twelve random training points were used. A novel composite solid was designed using 3D printing techniques that combined multiple base materials with distinct properties to achieve a spatial distribution of these materials within a representative volume element (RVE), arranged in a periodic lattice pattern.

In their study, Sharpe et al. [36] used the geometric projection technique to represent the struts in a lattice structure using the primitives of rods. To achieve a high stiffness-to-weight ratio, they developed a constrained Bayesian optimization (BO) framework for the design of micro-architectures (i.e., unit cells). Surrogate models approximated computationally expensive constraints, and the probabilities of satisfying the expensive constraints were incorporated as weights in the expected improvement function. A total of 13 design variables were considered in their study, which used two rods that were of equal diameter. Several interesting unit cell designs were identified using the BO framework that compared favorably to the popular octet truss design Deneault et al. [37].

In 2020, Gongora et al. [38] tested 600 distinct designs in triplicate using a grid-based experimental campaign. Based on the experimental data, simulations were conducted, and it was found that BO would reduce the number of experiments required by almost 60 percent. Longchao et al. [39] developed a data-driven framework to determine the optimal parameters for LPBF to achieve satisfactory surface roughness and dimensional accuracy. Under different combinations of process parameters, the framework integrates the Kriging model and the whale optimization algorithm (WOA) to find the optimal process parameters that achieve desired surface roughness and dimensional accuracy for as-built products. To determine the global optimal process parameters, the WOA was used. With optimized process parameters, LPBF parts with improved surface finish and dimensional accuracy were obtained, indicating that the optimized results are consistent with the experimental results.

Hazza et al. [40] employed a multi-objective genetic algorithm (MOGA) to minimize power consumption costs while taking into account factors such as cutting speed, feed rate, depth of cut, and rake angle. It was proposed by Iqbal et al. [41] that fuzzy rule-based systems could be used for multi-objective optimization. Kumar & Singh [42] proposed an optimization model that combined four performance characteristics using the utility concept based on Taguchi's design approach. To determine the Pareto front for multi-objective optimization, Kübler, Böhner & Steinhilper [43] developed an algorithm based on GA-based non-dominated sorting. The study analyzed resource consumption for multi-pass turning processes based on an a posteriori optimization process. For the evaluation and determination of optimal cutting parameters in a cutting scheme, Li et al. presented a multi-objective optimization model in 2015. A study conducted showed that the proposed model is effective in addressing the difficulties of machining sculptured parts and is more closely aligned with the characteristics of engraving and milling.

After going through the literature review, it is evident that:

1. Much work hasn’t been done in multi-objective optimization.
2. The papers used mostly artificial data.
3. The optimization method has a known function that is typically not available for manufacturing problems.

Table 2: A Summary of Prior Studies on Optimization in the Manufacturing Industry

Ref.	Year	Optimization method used	Focus
(AL Hazza et al., 2012)	2012	Multi-objective genetic algorithm	Minimize power consumption taking other factors into account
(Iqbal et al., 2013)	2013	Fuzzy rule-based system	Energy consumption, tooling costs, and productivity
(Kumar & Singh, 2014)	2014	Taguchi ' s approach and utility concept	Axial force, radial force, main cutting force and material removal rate
(Kübler, Böhner & Steinhilper, 2015)	2015	Meta-heuristic genetic algorithm	Resource consumption, machining time, and machining cost
(Amir et al., 2016)	2016	Bi-objective process optimization framework	Measured geometric accuracy in parts manufactured using fused filament fabrication
(Amir et al., 2018)	2018	Multi-objective accelerated process optimization	Optimizing mechanical properties of laser-based AM
(Sharpe et al., 2018)	2018	Constrained Bayesian optimization framework	Geometric projection to represent the struts in a lattice structure
(Asadollahi-Yazdi, Gardan & Lafon, 2018)	2018	Non-Dominated Sorting Genetic Algorithm-II (NSGA-II)	Production time and material mass
(Gongora et al., 2020)	2020	Grid based experimental campaign	Simulation data

2.3. Bibliometric Analysis

This study's primary objective is to identify primary research trends and areas of impact in the fields of optimization and manufacturing using bibliometric tools. Based on the Scopus database, 3107 articles were collected to achieve this objective. The most significant research areas were evaluated by using relevant keywords to conduct a comprehensive analysis of the current research trends. The area has also been identified and analyzed with respect to emerging research streams. The researchers extracted and analyzed bibliometric information from Scopus categories related to additive manufacturing, multi-objective optimization, and other related fields of study.

The Bibliometrix package in R [44] programming language has been used to analyze the results of the analysis. Through this approach, trends and patterns were examined within the dataset in detail, enabling easy identification of the most important research areas in the fields of optimization and manufacturing. Accordingly, this study provides valuable insight into the current state of research in these fields using bibliometric tools and an informed decision will be made using this knowledge.

A graphic representation of the trends in various research topics in each area, as well as the amount of work done in each area over the past few years, is shown in Figure 2. The figure illustrates how different research areas have evolved as well as the growth or decline in interest among researchers in various areas.

It is noteworthy that the figure highlights the emergence of multi-objective optimization as a trending topic in recent years. In recent years, this field of study has only recently gained recognition, suggesting that scholars and researchers are becoming increasingly interested in it.

Figure 2: The trending topics in the field in recent years

To analyze the set of publications, we used a word cloud, a graphical representation of the most used words and phrases. By employing this approach, we were able to gain insight into the most frequently used keywords or terms in a collection of articles about a particular research topic. It was possible to determine the relationship between the frequency of occurrence of each term and its importance by examining the size of each word in the word cloud.

The primary objective in creating the word cloud was to identify the most prominent keywords or terms relevant to the research topic from scholarly publications. The larger the font size of the word cloud, the more frequently used words are indicated, while the smaller the font size, the less frequently used ones.

As demonstrated in Figure 3, optimization, forecasting, and manufacturing were the most prominent words in the word cloud. Accordingly, these findings are in line with the journal's focus on these specific research areas, suggesting that scholars and researchers are interested in these

topics. In addition to providing a comprehensive overview of the range of topics discussed in the publications, the word cloud also allowed us to understand their relative importance.

There are several methods of analyzing a group of publications, and the use of a word cloud is only one of them. Other tactics may provide additional insight. It offers a quick and visual means of identifying the most important themes and trends in the dataset.

Figure 3: The world cloud showing the frequency of occurrence for the keywords

To gain a better understanding of the trend over time, the last step in the process involves analyzing the science publication data thoroughly. In Figure 4, the number of publications each year in the field of interest is presented. The plot indicates that the field is still in its early stages of development and has only recently begun to gain recognition. It is estimated that less than 500 articles are published each year, which is a relatively low number. One of the reasons for this may be a lack of funding, a lack of research interest, or an inability to obtain data.

Despite this low publication rate, it is important to note that it does not necessarily indicate a lack of progress or potential in the field. However, it may simply reflect the current state of research and development in the area. There is a possibility that the number of publications in this field will

increase significantly in the coming years due to further investment, increased interest, and technological advancements.

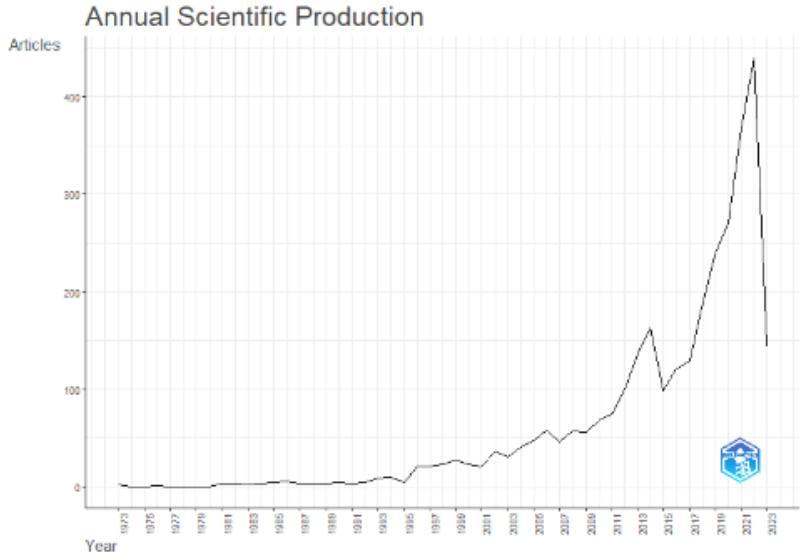

Figure 4: The annual scientific production in the field of study

3. Methodology

This section provides a brief explanation of the methods and terms used in this work, followed by a discussion of the data understanding.

3.1. Multi-objective Optimization

A multi-objective optimization is a practical method for solving problems that have conflicting objectives. An important advantage of this method is that it can optimize multiple objectives simultaneously while taking into consideration various equality and inequality constraints. It is important to emphasize, however, that no perfect solution can satisfy all objectives simultaneously. As an alternative, the goal is to identify a set of solutions, or the Pareto optimal set, in which each meets the objectives to an acceptable level without imposing a dominating influence on any of the others. An appropriate design vector must be selected for the specific project once this set of solutions has been selected by the decision-maker. Several mathematical formulations can be used to express the problem of multi-objective optimization, such as Alvarado-Iniesta et al. [45] in 2018:

Minimize (or maximize) $f(x) = [f_1(x), f_2(x), \ldots, f_m(x)]$ subject to the constraints

$$g(x) = [g_1(x), g_2(x), \ldots, g_p(x)] \leq 0 \text{ and } h(x) = [h_1(x), h_2(x), \ldots, h_p(x)] = 0. \quad (1)$$

where $x = [x_1, x_2, \ldots, x_n]$ is a vector of decision variables, $f_i(x)$ is the $i\text{-}th$ objective function, and $g_j(x)$ and $h_j(x)$ are the inequality and equality constraints, respectively. In most cases, it is impractical to identify a single solution, x , that can optimize all M objectives while adhering to all the constraints. Consequently, to assess objective vectors, it is common practice to apply Pareto domination.

3.2. Pareto Front

A non-dominated solution x^* is Pareto optimal if there does not exist another solution x' in S (let S be the solution space) such that $f_j(x') \leq f_j(x^*)$ for all $j = 1, 2, \ldots, m$ and $f_j(x') < f_j(x^*)$ for at least one j Natarajan et al. [46] , in 2019. The set of all Pareto optimal solutions is called the Pareto front, denoted as PF. Therefore, mathematically, PF can be expressed as:

$$PF = \left\{x^* \in S \mid \nexists x' \in S, x' \neq x^*, f_j(x') \leq f_j(x^*) \forall j = 1, 2, \ldots, m \wedge f_j(x') < f_j(x^*) \exists j\right\} \quad (2)$$

3.3. Bayesian Optimization

An optimization problem requires the identification of the global extremum, either maximum or minimum, of a mathematically defined function, known as an objective function in a particular area of interest Torn and Zilinskas, [47]. Optimization methods traditionally assume that the objective function is mathematically defined, which means that its analytical expression and gradient can be determined. Nevertheless, real-world problems usually involve situations in which the objective function is unknown, expensive to evaluate, noisy, and lacking analytical expression and gradient information. As a result, these functions are known as black-boxes Jones et al. [48], 1998. The budget for evaluating the black-box may be limited in some optimization scenarios, allowing for only a limited number of evaluations. As a result, it is imperative that each black-box evaluation be carefully selected to minimize the risk of regret. Using a surrogate model, the next point to be evaluated is chosen based on the predictive distribution of the objective function. Using the data collected from the black box, the model is iteratively trained. Shahriari et al. [49] in 2015 described how the model is trained iteratively. Using a probabilistic model, the input space is divided into points where objective function values are expected to be distributed. In this model, it is assumed that the objective function can be described by the probabilistic model, meaning that the model's assumptions about the objective function are correct. As previously mentioned, Bayesian Optimization (BO) is a type of approach used to find the optimal solution x^* for a black-box function $f(x)$: $x^* = \arg min_{x \in \chi} f(x)$, assuming the problem is for minimization. Bo is also represented by $\mathcal{A} = \left(\mathcal{M},\ \alpha(.), \mathcal{P}(f(x)|\mathcal{D})\right)$, where $f(x)$ is the function to be optimized, $\mathcal{M}$ is the surrogate model, $\alpha(.)$ Is the acquisition function, $\mathcal{P}(f(x)|\mathcal{D})$ is the predictive distribution x evaluation given the previous observation in dataset $\mathcal{D} = \{(x_i, y_i)|i = 1, \dots, t\}$ at iteration t.

Based on the prior distribution, BO suggests new points iteratively within the search space, and constructs an acquisition function to assess the probability of improvement at each point in the search space, representing the optimal tradeoff between exploration and exploitation. It is possible to acquire data by utilizing several acquisition functions, including Expected Improvement, Probability of Improvement, and Upper Confidence Bound. Following the acquisition of new data, the prior distribution is updated over time, and the process is repeated until the termination conditions have been met. The framework for the optimization is shown in figure 5.

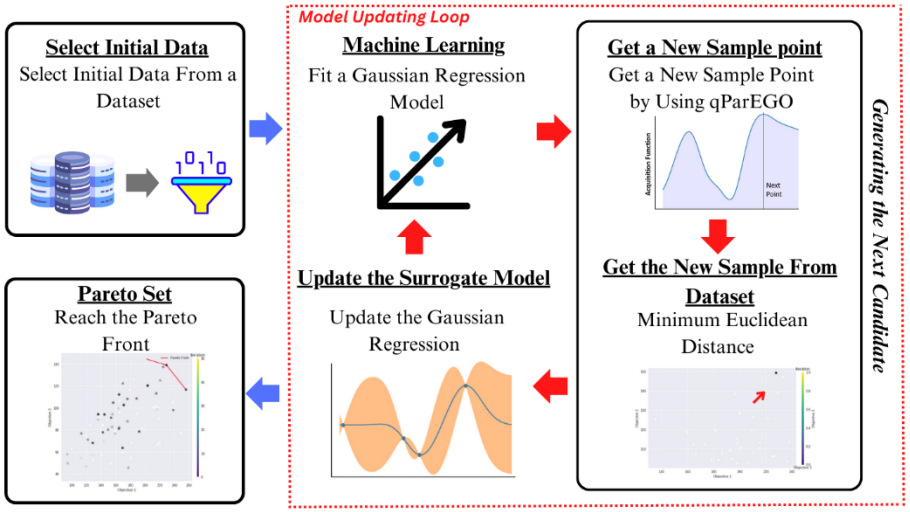

Figure 5: Multi-objective Bayesian optimization (MOBO) framework

Following is a summary of Bayesian optimization:

1. There is also a prior distribution that reflects any prior knowledge or assumptions about the objective function, which is typically modeled as a Gaussian process (GP). It is possible to add new information to the prior over time as it becomes available.
2. Using the prior, construct an acquisition function that measures the likelihood of improvement at each point in the search space. Among the most commonly used acquisition functions are Expected Improvement, Probability of Improvement, and Upper Confidence Bound.
3. Utilizing the acquisition function, select the next point to evaluate by balancing exploration of new regions of the search space with exploiting regions that contain the global optimum.
4. To calculate the new value, analyze the objective function at that point and add it to the observed value.
5. Update the prior distribution over the new data and repeat the process from step 2 until a satisfactory solution is reached. Iterations are conducted in the Bayesian optimization process.

3.4. Gaussian Process

Gaussian Processes (GPs) are a set of random variables with joint Gaussian distributions, with an infinite number of variables. Thus, GPs describe stochastic processes with joint Gaussian distributions at any number of input locations. GPs are essentially distributions over functions, which allows us to sample functions from them. Bayesian optimization (BO) can be modeled using the objective function as a sample from the GP. Due to its non-parametric nature, flexibility, and robustness, the GP is easy to estimate hyperparameters for, and does not overfit small amounts of data.

If we do not have any observations, we can also use GPs as a prior, which allows us to generate smooth functions without any observations. According to the GP prior, the possible values of a function at any given input location are given a mean (usually zero) and a standard deviation.

The Gaussian Process (GP) model can provide evaluations for both the predicted mean $\mu_t(x)$ and the epistemic uncertainty $\sigma_t(x)$ at any point x in the input space. The evaluations are derived from a specific set of observations $\mathcal{D}_{1:i} = \{(x_1, y_1), (x_2, y_2), \dots, (x_i, y_i)\}$, where x_i refers to the input variable of a process, while y_i refers to the corresponding output variable at time i (Greenhill et al. [50], 2020).

A GP can be fully described by its mean function $m(\boldsymbol{x})$ and covariance function $k(\boldsymbol{x}, \boldsymbol{x}')$:

$$f(\boldsymbol{x}) \sim \mathcal{GP}\big(m(\boldsymbol{x}), k(\boldsymbol{x}, \boldsymbol{x}')\big) \tag{3}$$

The covariance function of the GP receives two points as an input, x and x'. We define the prior mean function m (x) and the covariance function k(x, x') that computes the covariance between $f(x)$ and $f(x')$ must be evaluated as:

$$m(x) = \mathbb{E}[f(x)],$$

$$k(x, x') = \mathbb{E}[(f(x) - m(x))(f(x') - m(x'))] \tag{4}$$

Often, this function $k(\boldsymbol{x}, \boldsymbol{x}')$ is referred to as the "kernel", because it measures the smoothness of the process. It is generally expected that when two points $\boldsymbol{x}$ and $\boldsymbol{x}'$ are close, their corresponding process outputs $\boldsymbol{y}$ and $\boldsymbol{y}'$ will also be close, and the degree of closeness will depend on the distance

between the points rather than the exact location or direction of separation. In the case where we have a dataset $\mathcal{D} = \{((X_i, y_i)|i = 1, \dots, N)\}$, an experimental setting including observations with normally distributed noise $\varepsilon \sim N(0, \sigma^2_{\text{noise}})$. The observation model can be summarized as follows:

$$y = f(\boldsymbol{x_i}) + \varepsilon_i \tag{5}$$

Where ε_i = added noise. The GP builds a predictable distribution $p(f(x^*)|\mathcal{D})$ for the potential value of $f(x^*)$ at a new input point x^*. The build distribution is also Gaussian which is $p\left(f(x^*|\mathcal{D}) = \mathcal{N}\left(f(x^*)\middle|\mu(x^*), \upsilon(x^*)\right)\right)$. The GP prior mean is the prior knowledge of the problem, and it is typically set to 0. The mean and variance of the predictive distribution are given by:

where

$$\begin{aligned} \mu(\boldsymbol{x}^*) &= K_*^T[K + \sigma^2_{\text{noise}} I]^{-1} y, \\ \upsilon(x^*) &= k(\boldsymbol{x}_*, \boldsymbol{x}_*) - k_*^T[K + \sigma^2_{\text{noise}} I]^{-1} \boldsymbol{k}_* \end{aligned} \tag{6}$$

$$k = [k(\boldsymbol{x}, \boldsymbol{x}_1), k(\boldsymbol{x}, \boldsymbol{x}_2), \dots, k(\boldsymbol{x}, \boldsymbol{x}_t)]$$

$$\mathrm{K} = \begin{bmatrix} \mathrm{k}(\mathbf{x}_1, \mathbf{x}_1) & \dots & \mathrm{k}(\mathbf{x}_1, \mathbf{x}_\mathrm{t}) \\ \vdots & \ddots & \vdots \\ \mathrm{k}(\mathbf{x}_\mathrm{t}, \mathbf{x}_1) & \dots & \mathrm{k}(\mathbf{x}_\mathrm{t}, \mathbf{x}_\mathrm{t}) \end{bmatrix} \tag{7}$$

Covariance functions play a crucial role in determining our assumptions about the function we aim to learn Rasmussen [51]. These functions are used to measure the similarity between data points $X = (x_1, \dots x_N)^T$, and commonly used ones in GPs are the squared exponential and Mat´ern functions. Selecting the appropriate covariance function can significantly impact the outcome of a GP application, as each covariance function makes different assumptions about the target function. Therefore, it is essential to comprehend the fundamental properties and assumptions made by the most common GP covariance functions. In this thesis, we utilize the squared exponential (SE) function, also known as the radial basis function (RBF), which is a popular choice for the covariance function Greenhill et al. [52], 2020. The function is expressed as:

$$k(x\,, x') = \sigma_f^2 \exp\left(-\frac{r^2}{2l^2}\right) + \sigma_n^2 \delta_{pq} \tag{8}$$

Where the value of r represents the Euclidean distance between x and x'. while the length-scale parameter, denoted as l determines the smoothness of the functions generated by the Gaussian Process (GP). Typically, a different length scale l_j is utilized for each dimension j. The amplitude parameter or signal variance, represented by σ_f^2 f controls the range of variability of the GP samples. The noise variance, $\sigma_n^2\delta_{pq}$ is denoted by δ_{pq} and applies when the covariance function is calculated for the same point $k(x,x)$. The delta function δ_{pq} is used to model this condition.

3.5. Acquisition Function (qParEGO)

To determine the next experiment's most promising input settings, an acquisition function is utilized, which considers the Gaussian process model's predicted mean $\mu_t(\boldsymbol{x})$ and uncertainty $\sigma_t(\boldsymbol{x})$. In this thesis, the parallel efficient global optimization (qParEGO) serves as the selected acquisition function for the purpose. This approach aims to maximize the acquisition function to identify the most valuable input settings for the following experiment, considering both mean prediction and uncertainty

This is an extension of ParEGO which introduces parallelism for jointly optimizing and identifying the next best location, $\boldsymbol{x_{best,k}}$, in a batch setting where $\boldsymbol{X_{best,k}} = \{\boldsymbol{x_{best,k,1}}, \boldsymbol{x_{best,k,2}}, \dots, \boldsymbol{x_{best,k,q}}\}$, where k denotes the iteration number and q represents the batch size[53]. ParEGO is an advanced optimization algorithm that utilizes a global model to solve complex optimization problems with multiple objectives[53]. The EGO algorithm inspired ParEGO, which is an improved version of the former designed for optimizing a single objective [54]. Both EGO and ParEGO rely on surrogate models to guide the optimization of the black-box function, and this approach is known as the design and analysis of computer experiments (DACE)[55]. The primary concept behind the EGO algorithm is to use a surrogate model *F*, based on DACE, to approximate the objective function *f*. Then, an improvement criterion I ($\mathbf{x}$) is calculated using this model in the following manner [60].

$$\mathrm{I}(\mathbf{x}) = \begin{cases} f_{min} - \hat{f}(\mathbf{x}) & if\ \hat{f}(\mathbf{x}) < f_{min} \\ 0 & otherwise \end{cases} \tag{9}$$

The equation mentioned above includes two terms: f_{min}, which is the lowest evaluation obtained by f, and $\hat{f}(\mathbf{x})$, which represents the predicted value of the surrogate model F. The surrogate model F is assumed to be a Gaussian distribution with a mean of $\hat{f}(\mathbf{x})$ and a variance of $\hat{\sigma}^2(\mathbf{x})$. The

expected improvement EI (**x**) is defined as the expected value of I (**x**) which is given by the following equation [5].

$$\text{EI}\ (\mathbf{x}) = \mathbb{E}_{\text{F}(\mathbf{x})}[\text{I}\ (\mathbf{x})] \tag{10}$$

When the DACE model is built using Kriging, the expected improvement can be expressed using the following equation.

$$\text{EI}\ (\mathbf{x}) = \begin{cases} \left[f_{min} - \hat{f}(\mathbf{x})\Phi\left(\frac{f_{min}-\hat{f}(\mathbf{x})}{\sigma_k(\mathbf{x})}\right)\right] + \left[\sigma_k(\mathbf{x})\phi\left(\frac{f_{min}-\hat{f}(\mathbf{x})}{\sigma_k(\mathbf{x})}\right)\right] & if\ \sigma_k(\mathbf{x}) > 0 \\ 0 & if\ \sigma_k(\mathbf{x}) = 0 \end{cases} \tag{11}$$

Here, Φ and ϕ refer to the cumulative distribution and probability density functions of a Gaussian distribution with a mean of zero and variance of one. Maximizing the expected improvement results in the selection of the next parameter set for evaluating the function f. This maximization process involves balancing the reduction of the approximation error in the DACE model with a sufficient decrease in the objective function. To optimize multiple objectives, the ParEGO algorithm first combines all objectives linearly to convert the problem into a mono-objective optimization problem. An iteration of the EGO method is then applied to this problem. During every iteration of the algorithm, a random weight vector λ^j is generated using the following definition.

$$\lambda^j = \{\lambda_1^j, \lambda_2^j, \dots, \lambda_n^j\} \mid \lambda_k^j \in [0,1] \quad \forall k = \{1,2,\dots,n\} \ \ and \ \ \sum_{k=1}^{n} \lambda_k^j = 1 \tag{12}$$

The equation presented above is utilized by the Tchebycheff function f_λ^j, which linearly combines the objectives as shown below.

$$f_\lambda^j(\mathbf{x}) = \max_{k=1,2,\dots,n}\left(\lambda_k^j f^j(\mathbf{x})\right) + \rho \sum_{k=1}^{n} \lambda_k^j f^j(\mathbf{x}) \tag{13}$$

The constant ρ is set to a value of 0.05 [56]. The optimal points obtained from several mono-objective optimizations are then utilized to determine the Pareto Front. The qParEGO approach reduces the computational effort and can be particularly advantageous when time is a critical factor in conducting expensive evaluations in batch [57].

3.6. PHV

This metric is used to evaluate the quality of a Pareto front approximation in multi-objective optimization. In this metric, the proportion of the HV enclosed by the true Pareto points is calculated in the resulting Pareto points Aboutaleb et al. [58].

$$PHV = \frac{HV(\ Resulted\ Pareto\ Points\ )}{HV(\ True\ Pareto\ Points\ )} \tag{14}$$

PHV is a measure within the range of [0, 1], and in an ideal case, PHV is equal to 1.

3.7. Proposed MOBO Method for Optimization

In this section, a new version of data-driven multi-objective Bayesian optimization (MOBO) approach is presented. The proposed method consists of four main phases: Initialization, Candidate Generation, Optimization, and Epsilon

3.7.1 First stage

As part of the preparation process for this thesis, the dataset is divided into two separate sets - a training set and a testing set. The training set, which comprises 70% of the data, will be used to initialize and train the algorithm, while the remaining 30% will be used to evaluate the accuracy of the model based on new, unseen data. By doing so, we ensure that the algorithm does not overfit the training data and can generalize well to new observations.

3.7.2. Initialization

As a first step in the process, a set of specific input criteria is established, including the number of iterations, the size of the initial dataset, and the search space for hyperparameters. It is important to note that these criteria are selected in accordance with the problem being addressed and the desired optimization outcomes. There is always one sample generated in each iteration. A random dataset is generated after these criteria are defined to model the behavior of the objectives. After the dataset has been collected, a Gaussian process (GP) surrogate model is fitted using this data. As a result of the GP, a function can be created that can estimate both the objective values and their uncertainties based on the data. As a result of utilizing the surrogate model, the optimization process can make informed decisions about which points to evaluate next, to find the optimal solution in the end.

3.7.3. Generating the Next Candidate

The next step is the calculation of the acquisition function score based on the GP surrogate model. To accomplish this, the expected improvement of each objective is integrated over the hypervolume of the region dominated by the current Pareto set. Afterward, the point with the highest EI score will be chosen as the candidate for the new sample point, which is expected to be outside of the current dataset. It is determined by calculating the Euclidean distance between the new candidate and all the existing points in the dataset that are closest to the new candidate. To further refine the predictive capability of the GP model, the closest point is considered a new sample and is used to update the GP model. After each iteration, the process is repeated until the optimal solution is obtained, as determined by a predetermined stopping criterion, such as the number of iterations or the level of performance acceptable to the customer. To optimize multiple objectives while minimizing function evaluations, the GP surrogate model and acquisition function is utilized.

3.7.4. Model Updating

Steps one and two are repeated until the predetermined number of iterations has been reached after selecting the new sample point and updating the GP surrogate model. Iteratively, the GP model is updated by choosing new points to evaluate based on a balance between exploration and exploitation. Exploring new regions of the search space can lead to the discovery of new solutions, but exploitation of existing knowledge will assist in identifying the most appropriate solution as well. An analysis of the Pareto front of the resulting set of samples is conducted following the optimization process. In the Pareto front, there are only non-dominated solutions, which means that any improvement in one objective can only be achieved at the expense of another. This process is repeated until the stopping criteria have been met, with the resulting data being collected and stored for prediction purposes after each iteration. Using this approach, it is possible to optimize several objectives efficiently while simultaneously generating useful data which can be used to facilitate future decision-making. The optimization flowchart can be seen in Figure 6.

3.8. Design of Experiment (DOE) Method

Design of experiments (DOE) is a statistical method used to organize and carry out experiments. It is used to identify the variables that influence the results of an experiment and to ascertain how

these variables are related. DOE can aid in minimizing experimental error and maximizing the information learned from an experiment.

3.8.1. Latin Hypercube Sampling (LHS)

Latin hypercube sampling (LHS) is a DOE technique for obtaining a sample of plausible parameter combinations from a multidimensional space. Compared to other random sampling techniques, LHS ensures that the chosen parameter combinations uniformly distribute and effectively cover the complete range of the variables of interest.

DOE and LHS are complementary methods that can be used together to optimize the experimental design process. DOE allows to determine the factors and levels to be tested and provides a structured framework for conducting experiments. Contrarily, LHS aids in choosing a subset of parameter combinations from the complete range to be evaluated, ensuring effective parameter space coverage.

Combining DOE with LHS allows to choose a subset of trials that offers a representative and uniformly distributed sample over the parameter space, thus optimizing the experimental design. With the aid of this strategy, fewer experiments are needed, more time and resources are saved, and the statistical power of the analysis is improved.

3.8.2. LHS Procedure

1. For each sample calculate the Euclidean distance between the sample and all records in the dataset and append the calculated distances to a list.
2. Create a Linear Regression model and fit the model to the data using the features and objectives.
3. Get the coefficients (slopes) and the intercept of the linear function used for each objective.
4. Define the two functions to maximize and generate Latin hypercube samples.
5. Get the Pareto front which is a point not dominated by any other point.

3.9. Proposed Epsilon-Greedy Method for Prediction

In this section, the proposed method for the prediction is discussed. The epsilon greedy is described first which is utilized for the data collection. The collected data will be used for training the ML based prediction models. Then the prediction model utilized is discussed followed by the evaluation criteria used for performance assessment.

3.9.1. Epsilon-Greedy

The Epsilon greedy model is used to maintain balance in the data collected or experiments conducted for prediction. As a result of this approach, it will be possible to ensure that the collected data is diverse and representative of the entire dataset. First, a value of epsilon (0-1) needs to be decided before the sequential experiments. Then, a random number between 0 and 1 is generated. A conditional statement is used to generate a new sample point. The algorithm will use the previously described approach (exploitation) if the random number exceeds a predefined threshold (e.g., 0.2). However, if the random number is less than the threshold, the algorithm will choose features and objective values using a randomly selected index from the dataset. Because of this approach, the resulting data is not biased towards a particular subset of the dataset, making it more suitable for predicting future events. Our objective is to generate a diverse and balanced set of data that can be utilized for the training of different predictive machine learning models. The framework for the Epsilon greedy approach is presented in Figure 7.

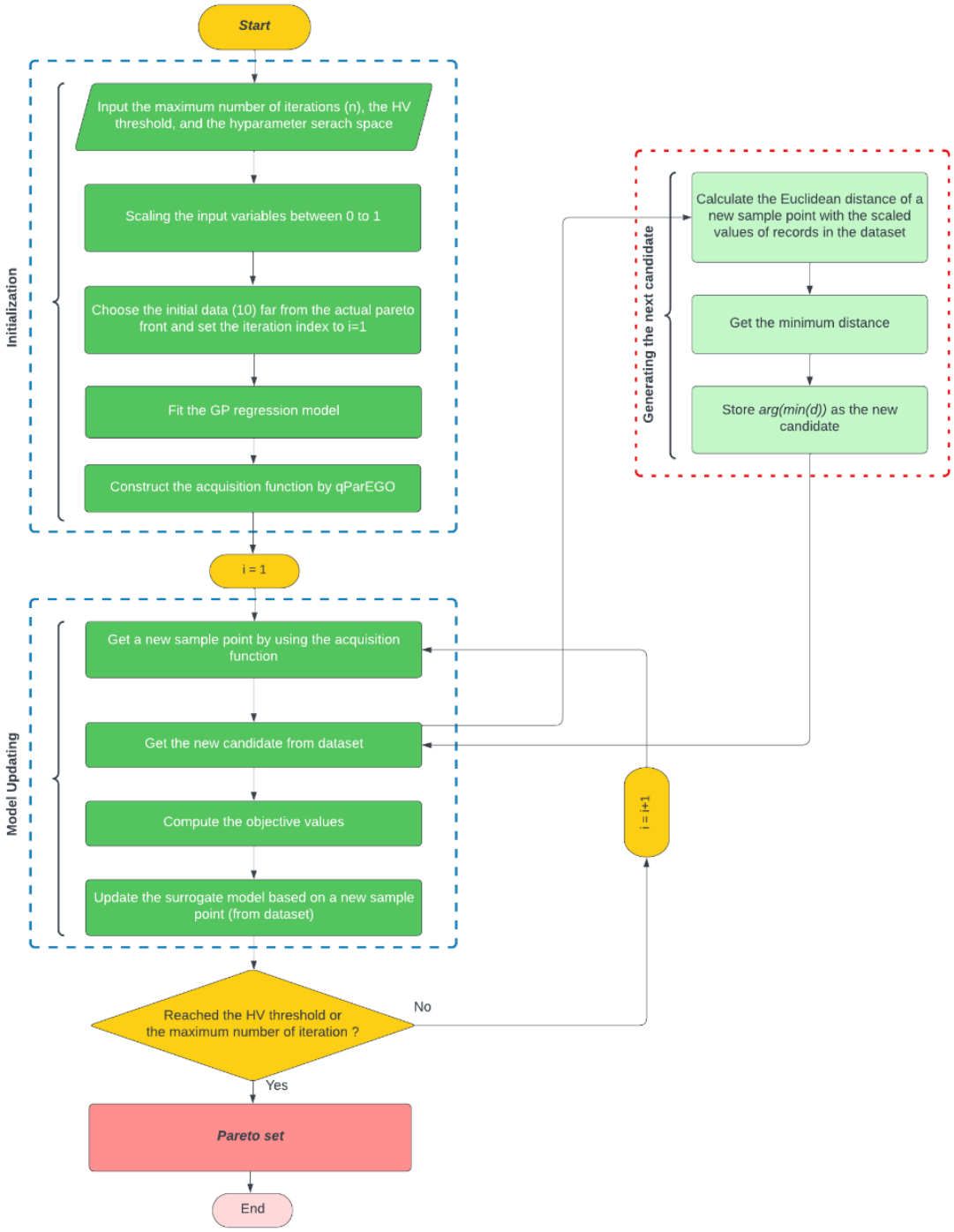

Figure 6: The optimization flowchart

3.9.2. Prediction and Comparison

A new training dataset will be created by following the proposed prediction framework. Various prediction algorithms will be then fitted to this dataset including Linear Regression, Random

Forest, and Lasso Regression. The performance of these algorithms is evaluated on a test dataset which is kept aside from the beginning for the evaluation purpose. We compare the performance of the proposed epsilon-greedy framework by comparing with other training mechanisms such as DOE based training and random sampling. For DOE based training, we generate a training set using LHS approach. On the other hand, for the random sampling, we just randomly generate the training dataset. However, we made sure all of these training datasets contain similar amount of data points and they are tested on the same test set.

3.9.3 Performance Evaluation

To evaluate the precision of the predictive model, various metrics were employed, namely the root mean squared error (RMSE), and the coefficient of determination (R2). These error measurements are defined based on;

$$RMSE = \sqrt{\sum_{i=1}^{n} \frac{(\hat{y}_l - y_i)^2}{n}}$$

$$R^2 = 1 - \sum_{i=1}^{n} (\hat{y}_l - y_i)^2 / \sum_{i=1}^{n} (\bar{y}_l - y_i)^2$$

The notations: $\hat{y}_l$, represents the predicted value, represents the observed value, and¯denotes the mean of the observed values.

The RMSE serves as a gauge for the proximity between the predicted and observed values. A smaller RMSE indicates a closer alignment between the two. In essence, it quantifies the average magnitude of the differences between the predicted and observed values.

The coefficient of determination (R2) illuminates the percentage of variation in the response that can be explained by the model. When R2 approaches 100%, it signifies that the model can account for a significant portion of the variability present in the data. This metric serves as a measure of how well the model captures and describes the underlying patterns and relationships within the dataset. By incorporating these error metrics, we can comprehensively assess the accuracy and performance of the predictive model, enabling a deeper understanding of its predictive capabilities and the degree to which it accounts for the observed data's variability.

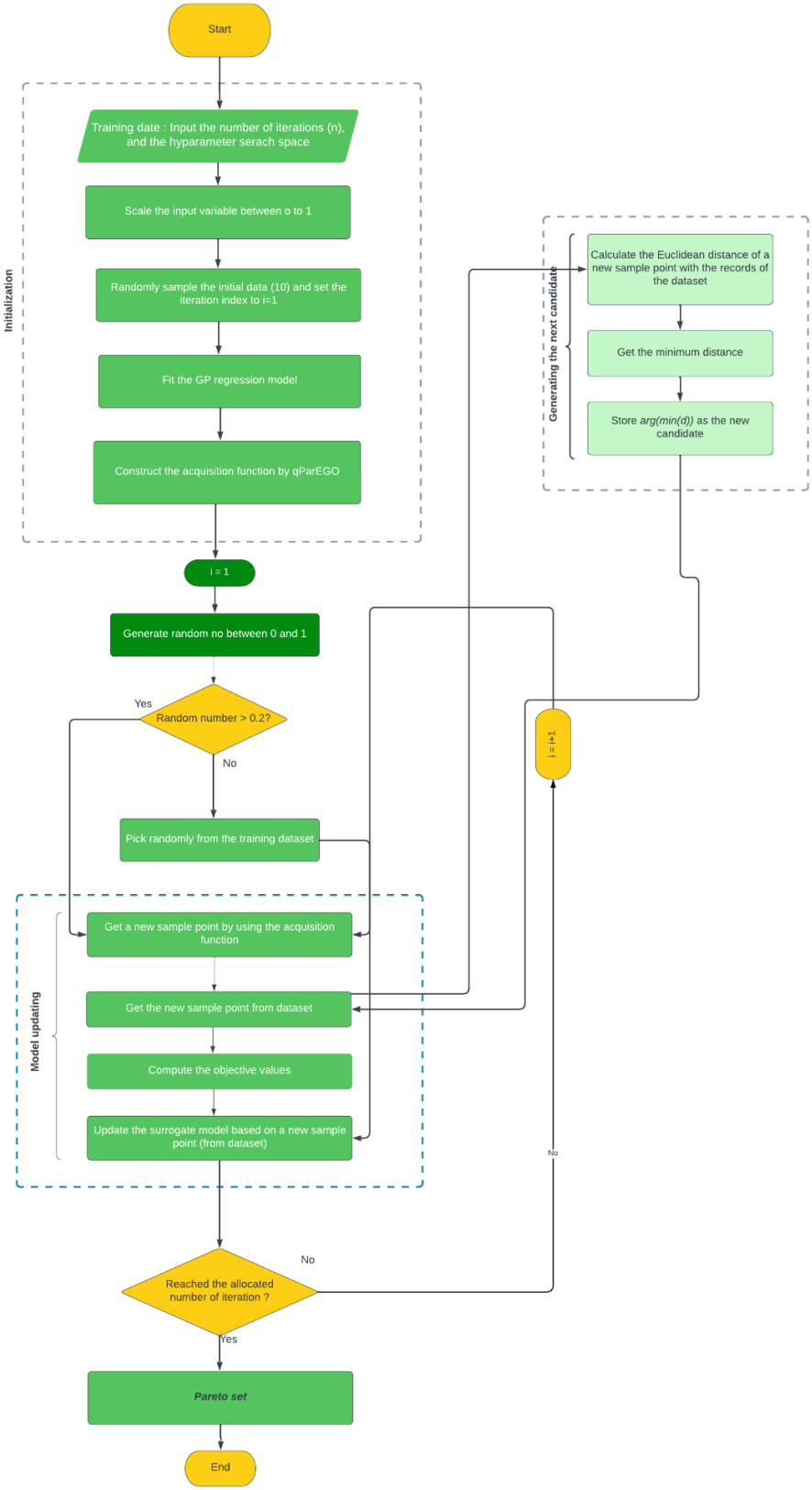

Figure 7: Epsilon greedy framework

By using the proposed approach, we can generate a wide range of data and then select the most appropriate predictive model based on the results. The flowchart for the prediction method is presented in Figure 8.

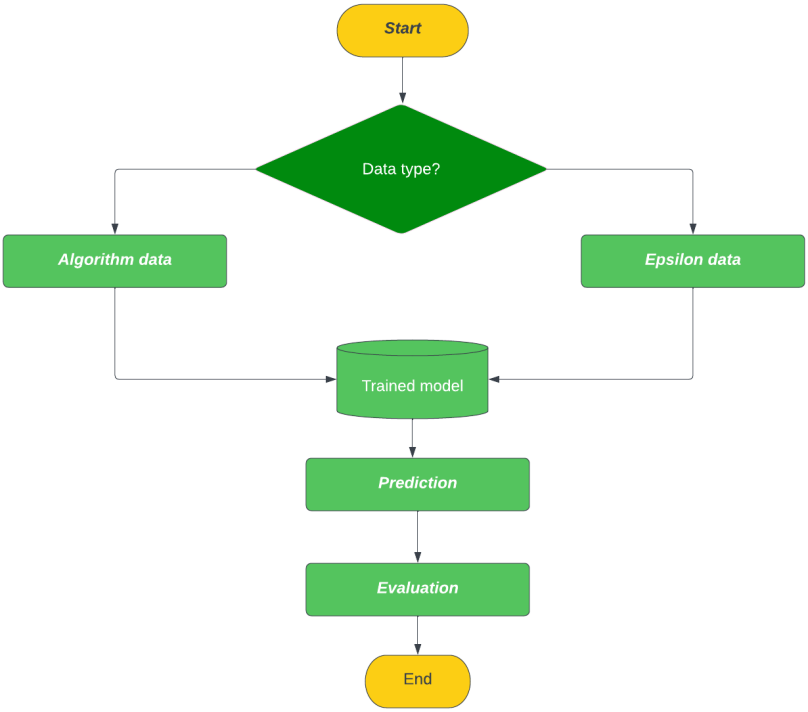

Figure 8: The flowchart for the machine learning prediction

4. Data Understanding

In this project, the proposed optimization and Epsilon-greedy framework are applied to two different datasets. The first dataset is an AM dataset with 25 experimental data augmented artificially by four hundred percent. The other dataset is experimental data found online for a material design problem. Both data are used to settle the bias that might arise from having seventy-five percent of the AM data being artificial.

4.1. Data Understanding for DED Data

A Bayesian optimization model framework has been applied to the data. The data consists of 25 data points with three features and two objectives. The features consist of laser power, scanning speed, and layer thickness. Those objectives are elongation and ultimate tensile strength (UTS). A variety of transformations are applied to the existing dataset to enhance the original data. Python is used to implement the Image Augmentation Library (imgaug). The purpose of data augmentation is to increase the size of an existing dataset by generating new samples like the existing ones. By doing so, machine learning models can perform better. Four augmentation techniques are employed in the pipeline: flipping the data upside down, flipping the data left to right, applying affine transformations (scaling, translation, and rotation), and adding Gaussian blur. A new sample is generated by applying the augmentation pipeline to the existing data. To accomplish this, a Python function called "aug_pipeline (images=existing_data)" is used. The resulting new data is then concatenated with the existing data to create a new dataset. Lastly, the new augmented data is saved to a file which can be used as input to a machine learning algorithm. The data augmentation flowchart is shown in Figure 9.

4.2. Data Understanding for the MDS Data

For the MDS data, we have applied our multi-objective Bayesian optimization model framework to explore the MAX ternary carbide/nitride space through Density Functional Theory (DFT) calculations. $M_{n+1}AX_n$, or in short MAX phases are layered, hexagonal, early transition metal carbides and nitrides. M represents a transition metal, A represents group IV and VA elements in the periodic table, and X represents either Carbon or Nitrogen [59], 2013. The coexistence of metallic and metallic/covalent linkages inside the layered structures of the MAX phases gives these materials a range of properties between those of ceramics and metals [59], [60],[61]. Despite the

fact that only a small portion of the pure ternary MAX phase composition palette has been synthesized to date, there are significant opportunities to discover promising chemistries with optimal property sets by considering different stacking sequences and deviations from stoichiometric ratios at the M, A, and X sites [62], 2018. MAX phases are a suitable material system for testing simulation-driven frameworks for materials discovery due to their diverse chemistry and the broad range of property values [63] 2014. We have used the MAX phases whose MDS consists of M_2AX and M_3AX_2 stoichiometries in our model framework. The MDS consists of a total of 403 MAX phases and in this work, our objective is to identify the materials with the maximum bulk modulus (K-exp) and maximum shear modulus ($G - exp$). Maximizing both shear modulus and bulk modulus can result in a material with high stiffness, which means that it will deform very little under stress. This is typically desired for applications where high strength and stability are important, such as in construction materials, aircraft structures, and medical implants. Like most other sequential learning approach, in this work, we assumed that we have some prior knowledge of the MDS of the MAX phases. This knowledge is available for the initial experiments before starting to conduct the sequential experiments. We expressed this prior knowledge as a set of input features that possess some relationships with the desired properties we are looking for. In 2018, Talapatra et al. [64] considered a list of features to represent each candidate of the MAX phase with the help of their domain knowledge and a thorough review of the literature. We followed the dataset, which was used in their work, however, we worked with different sets of features and followed different goals. The following table mentions all the initial features with their description which have an impact on the material properties of the candidates in the MAX phase.

Table 3: Input features with description

Feature	Description
C	Empirical constants.
m	
C_v	Valence electron concentration
$\frac{e}{a}$	Electron to atom ratio
a	Lattice parameters
c	
Z	Atomic number
$E - exp$	Young modulus
I_{dist}	Interatomic distance
Col_M	

Col_A	The groups according to the periodic table of the M, A & X elements
Col_X	
O	The order of MAX phase (whether of order 1 corresponding to M_2AX or order 2 corresponding to M_3AX_2)
APF	Atomic packing factor
rad	Average atomic radius
vol	Volume/atom

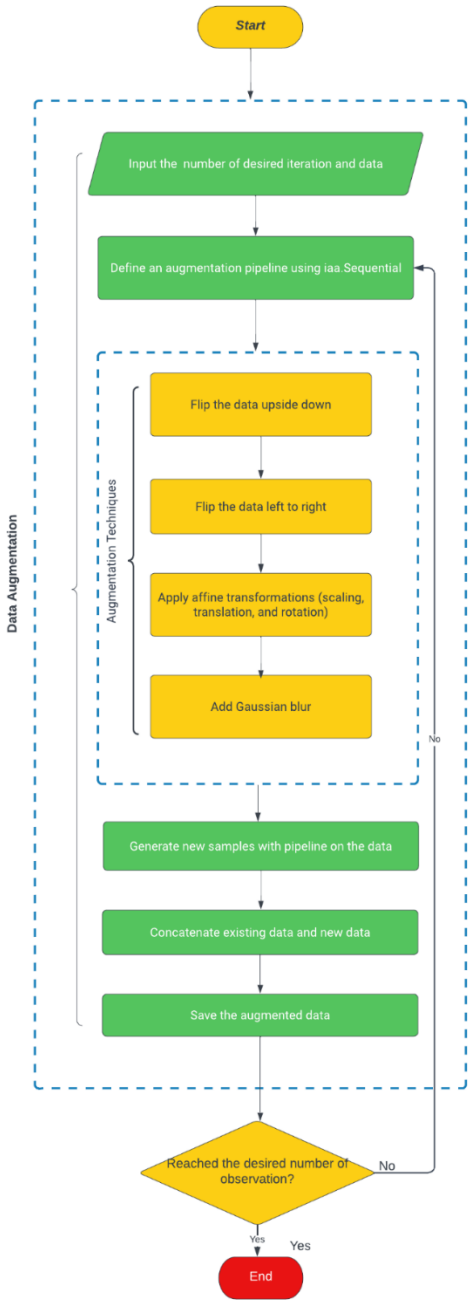

Figure 9: The data augmentation flowchart

5. Results

This section presents the case studies to test our model for both optimization and prediction tasks. The research used two different cases to test the validity of the proposed frameworks. For both cases, first, optimization is performed to obtain a high-quality Pareto front with a minimal number of data points. These optimization results are compared with the DOE approach. Secondly, machine learning models such as linear regression, random forest regressor, and Lasso regressor are trained using our proposed epsilon-greedy approach, DOE approach, and random sampling, and a comparison is made based on the test results.

5.1. Analysis of the Optimization Model

In this section, we discussed the outcome of our proposed optimization approach, the result and compared it with the DOE approach for two cases.

5.1.1. Case-1: Material Design Space Data

This section presents the first case study to test our proposed MOBO model. We performed the optimization sequentially using the proposed multi-objective optimization model and compared the result to the design of experiment approach in terms of the hypervolume (HV).

To apply the proposed optimization model, it is necessary to establish certain initial parameter values. The key parameters of the algorithm are listed in Table 4.

Table 4: The primary parameters of the proposed MOBO approach for the MDS data

Parameter	Description	Value(s)
b	Batch size	5
n	Maximum number of iterations	150
$NUM\_RESTARTS$	The number of random restarts to perform when optimizing an acquisition function	10
$RAW\_SAMPLES$	The number of random samples to generate from a given search space	400
$standard\ bounds$	The lower and upper bounds of a search space (a tensor)	[0,1]
$MC\_SAMPLES$	The number of Monte Carlo samples to use when estimating the expected improvement	32
k	Number of initial samples	10
l	Number of records in the dataset	402
hv	The HV threshold	0.97

Some of the parameters utilized in the model are adapted based on Botorch (Balandat et al., 2020) and primarily used during the optimization phase. However, other parameters, such as k, l, and n, are determined based on the characteristics of the dataset and the specific cases presented in this research. For instance, to reduce manufacturing costs, we limit the amount of data utilized to obtain the Pareto front to no more than one-third of the entire data. Additionally, we aim to achieve a hypervolume of at least 0.97.

Now, we evaluate the model's performance by conducting 25 runs on the model and analyzing the Pareto front. We investigate the convergence behavior of the best, worst, and median runs of the model using the proportional hypervolume.

Furthermore, we provide an in-depth analysis of the proposed model's procedure for the median run. This analysis highlights how the model utilizes an initial sample, deliberately positioned far from the Pareto front, to optimize both objectives and obtain a Pareto front. Figure 10 presents the box plot of the runs. The PHV values range from 0.92 to 0.97, which shows a great result as it did not deviate much from the threshold set.

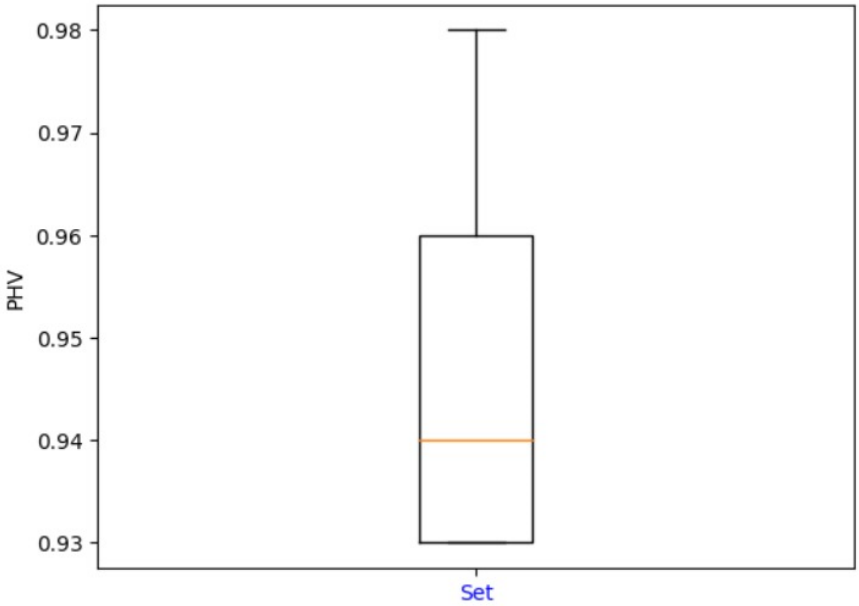

Figure 10: The stability of the model based on PHV in different runs

Figure 11 shows the convergence towards the Pareto front for the best, median, and worst runs using the number of iterations as the x-axis and IGD criteria as the y-axis. In addition, it is

noteworthy that the best run has the highest convergence rate, with the Pareto front being achieved in approximately 40 iterations.

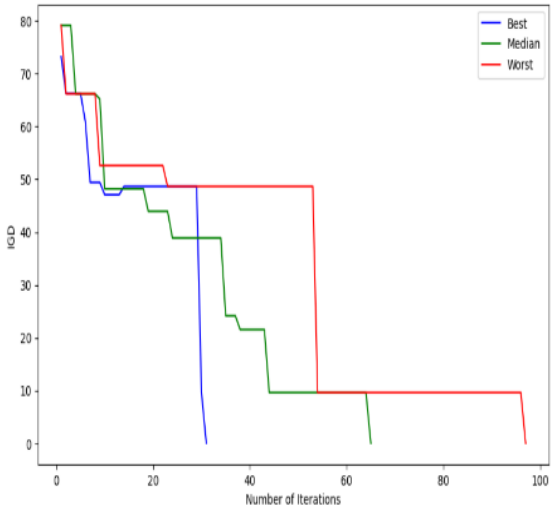

Figure 11: Convergence behavior of best, median, and worst run of the model based on IGD criterion

Figure 13 illustrates the progression of the optimization model. An evaluation of the sample status at different stages of the optimization process is presented in this figure, which shows the sample status after the first iteration, the sample status after half of the total iterations, as well as the final Pareto front. We are able to get the pareto front after 149 iterations. This is about 40% of the entire dataset.

First Iteration	**50% of the Iteration**	**Pareto Front**

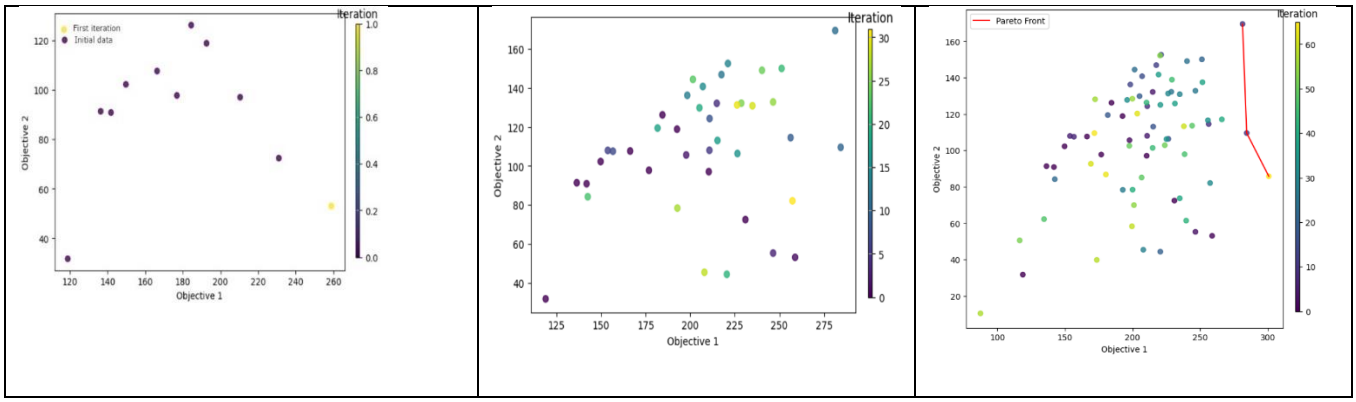

Figure 12: Proposed method for the MDS datasetshowing a) the starting point b) at 50% c) the full optimization

Table 5 summarizes the key performance metrics of the MOBO process at different stages of the optimization. These metrics are essential for evaluating the effectiveness and efficiency of the MOBO method.

The hypervolume achieved at the final iteration is a crucial indicator of the optimization process's quality. A value closer to 1 represents superior performance. In our study, we observed hypervolumes of 0.53, 0.93, and 0.97 at the beginning, middle, and end of the optimization, respectively. These values suggest that the optimization process progressively improved over time, with the final iteration demonstrating the highest hypervolume, indicating a substantial enhancement in the quality of the optimized solutions.

The proportional hypervolume metric provides a normalized measure of the hypervolume achieved relative to a predefined reference point. Our findings revealed proportional hypervolume values of 0.55, 0.93, and 1 at the beginning, middle, and end of the optimization process. These results indicate a significant improvement in the optimization quality, with the final iteration achieving the maximum proportional hypervolume, implying that the optimization method effectively explored the solution space and approached the reference point more closely.

The generational distance (GD) metric quantifies the average distance between the generated solutions and the true Pareto front. Lower values indicate better convergence. Throughout the optimization, the generational distance exhibited a substantial reduction, declining from 83.4 at the beginning to 0.0054 at the middle, and further improving to 0.0052 by the end. These

diminishing values indicate an increasingly accurate approximation of the true Pareto front, reflecting the optimization method's ability to converge towards the optimal solutions.

The inverted generational distance (IGD) measures the average distance between the true Pareto front and the closest generated solution. Similar to the generational distance, lower values represent better convergence. In our study, the inverted generational distance decreased significantly from 79.2 at the beginning to 9.61 at the middle, and ultimately reached a highly favorable value of 0.005 at the end of the optimization process. These results further confirm the optimization method's ability to approximate the true Pareto front, with the final iteration exhibiting an exceptional proximity to the optimal solutions.

Overall, the results presented in Table 5 demonstrate the continuous improvement and convergence of the proposed process. The achieved hypervolumes, proportional hypervolumes, generational distances, and inverted generational distances serve as objective measures of the optimization method's efficacy, illustrating its ability to explore the solution space, approach the reference point, and approximate the true Pareto front.

Table 5: Reuslt for the MDS data

First Iteration	**50% of the Iteration**	**Pareto Front**
Hypervolume = 0.53	Hypervolume = 0.93	Hypervolume = 0.97
Proportional Hypervolume = 0.55	Proportional Hypervolume = 0.93	Proportional Hypervolume = 1
Generational Distance = 83.4	Generational Distance = 0.0054	Generational Distance = 0.0052
Inverted Generational Distance = 79.2	Inverted Generational Distance = 9.61	Inverted Generational Distance = 0.005

Figure 13 compares the hypervolume of two approaches: the Latin hypercube method using the design of experiment (DOE) approach, and the proposed approach. Hypervolume is a performance metric, with a value closer to 1 indicating better model performance. The proposed approach achieved a significantly higher hypervolume of 0.97 compared to the DOE approach's value of 0.79.

This difference in hypervolume values clearly demonstrates the efficacy and advantages of our novel approach. By attaining a hypervolume of 0.97, the proposed approach was able to achieve more comprehensive coverage of the objective space, leading to better overall results than the DOE approach. The improved performance of the proposed approach is due to its innovative techniques

and enhancements. These advancements enable the method to efficiently explore the design space, effectively identifying optimal solutions and maximizing the hypervolume.

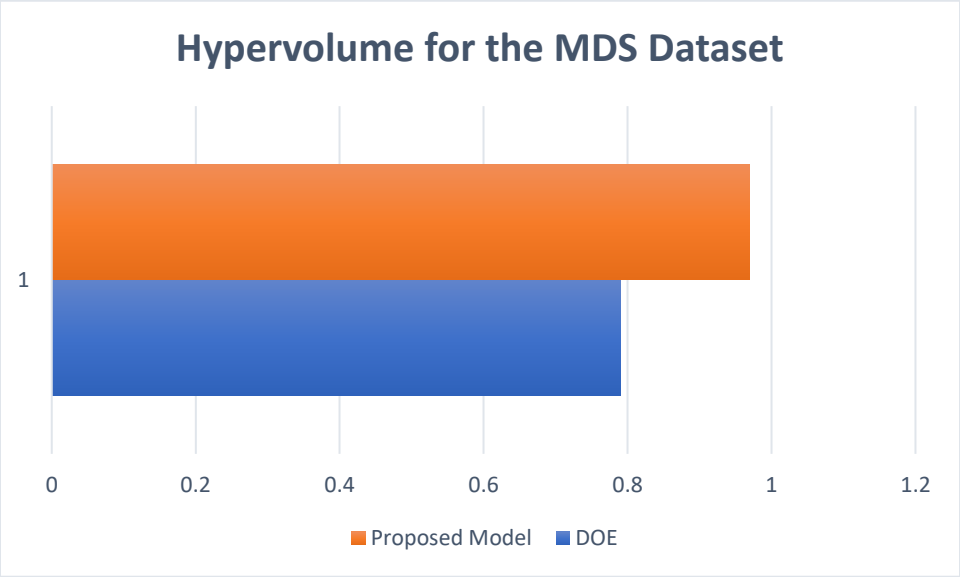

Figure 13: Hypervolume for the different approaches for the MDS data

The substantial difference in hypervolume values indicates that the proposed approach is a significant improvement over the traditional DOE method. Researchers and practitioners seeking to optimize their models and obtain superior results should consider implementing the proposed approach.

In summary, Figure 13 shows that the proposed approach achieved a significantly higher hypervolume than the DOE approach, demonstrating its superiority in achieving comprehensive coverage of the objective space and obtaining optimal solutions. These findings affirm the effectiveness and superiority of the proposed approach in improving model performance and results.

5.1.2. Case 2: The DED data

This study employed the proposed MOBO approach to optimize the parameters for the DED dataset. The section used two different datasets, the first part is focusing on both the original dataset comprising 25 data points and the second part is for the augmented dataset consisting of 100 data points. Our optimization process began by optimizing the parameters for a subset of 5 data points, as demonstrated in Figure 14a.

Table 6: The primary parameters of the proposed Epsilon-greedy approach for the DED data

Parameter	Description	Value(s)
b	Batch size	5
n	Maximum number of iterations	15
$NUM\_RESTARTS$	The number of random restarts to perform when optimizing an acquisition function	10
$RAW\_SAMPLES$	The number of random samples to generate from a given search space	25
$standard\ bounds$	The lower and upper bounds of a search space (a tensor)	[0,1]
$MC\_SAMPLES$	The number of Monte Carlo samples to use when estimating the expected improvement	32
k	Number of initial samples	10
l	Number of records in the dataset	402
hv	The HV threshold	0.97

The parameters used is shown in Table 6, to initiate the optimization process, we selected a subset of 5 data points from the original dataset as demonstarated in figure 14 a. We carefully chose the parameter settings to effectively explore the search space and guide the optimization process towards finding optimal solutions. Our objective was to simultaneously optimize multiple objectives, considering their respective trade-offs and dependencies.

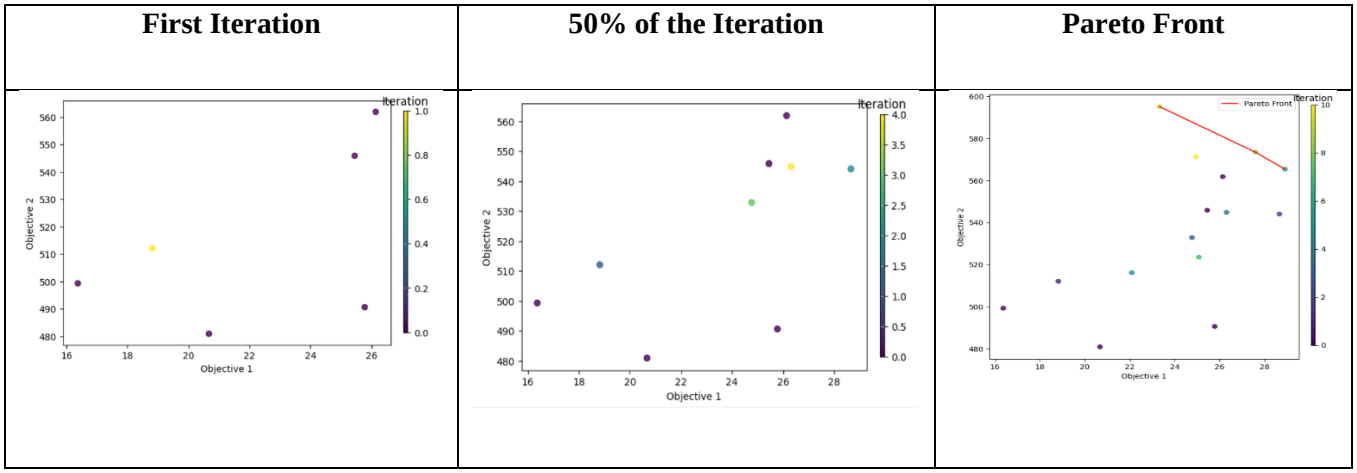

Figure 14:Proposed method for the DED datasetshowing a) the starting point b) at 50% c) the full optimization

We recorded and analyzed various metrics throughout the optimization process to assess the progress and convergence of the algorithm as shown in figure 14c. These metrics included convergence plots, objective function values, and performance indicators such as hypervolume and generational distance. By monitoring these metrics, we gained valuable insights into the algorithm's behavior and its ability to explore the search space effectively.

Overall, the multi-objective Bayesian optimization process yielded promising results in optimizing the parameters for the DED data. The obtained set of Pareto-optimal solutions is attained with 15 datapoint out of the actual 25.

Table 7: result for the DED data

First Iteration	**50% of the Iteration**	**Pareto Front**
Hypervolume = 0.84	Hypervolume = 0.92	Hypervolume = 0.98
Proportional Hypervolume = 0.87	Proportional Hypervolume = 0.95	Proportional Hypervolume = 1
Generational Distance = 21.7	Generational Distance = 21.7	Generational Distance = 2.6
Inverted Generational Distance = 4.4	Inverted Generational Distance = 15.5	Inverted Generational Distance = 2.7

In table 7, the hypervolume and proportional hypervolume both increase as the optimization progresses, indicating that the Pareto front approximation is becoming better and more diverse. The generational distance decreases as the optimization progresses, indicating that the Pareto front approximation is becoming closer to the true Pareto front. The inverted generational distance increases as the optimization progresses, also indicating that the Pareto front approximation is becoming closer to the true Pareto front.

Overall, the results of the multi-objective Bayesian optimization process are promising. The Pareto front approximation is becoming better, more diverse, and closer to the true Pareto front as the optimization progresses. Due to limitations in generating and utilizing the original dataset for the DOE approach, we were unable to employ it in our analysis. As a result, we solely utilized the augmented dataset for our investigation with the DOE approach.

The augmented dataset, consisting of a larger quantity of data points, presented an opportunity to overcome the constraints of the original dataset. By exclusively focusing on the augmented data, we aimed to leverage its increased size to compensate for the unavailability of the original dataset in the context of the DOE approach.

We followed a similar procedure for the augmented dataset to what we did with the original data, but with a slight modification. The augmented dataset was larger than the original data, so we started with 10 data points instead of 5. This allowed us to explore a wider range of parameters and refine the optimization process.

By starting with 10 data points, we were able to leverage the increased amount of information available to guide the parameter optimization. This larger initial subset provided a more representative sample of the augmented dataset and allowed us to capture its underlying characteristics more effectively.

First Iteration	50% of the Iteration	Pareto Front
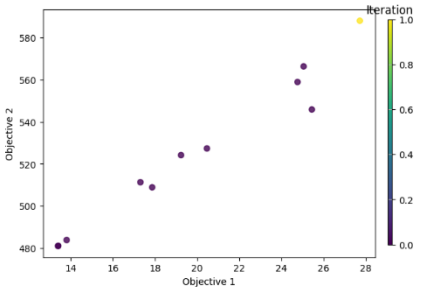	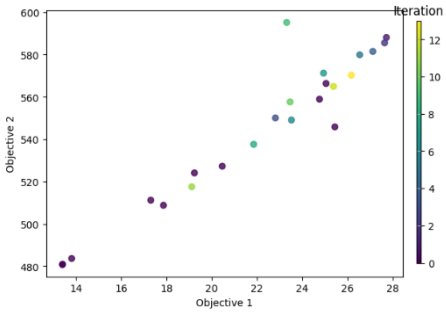	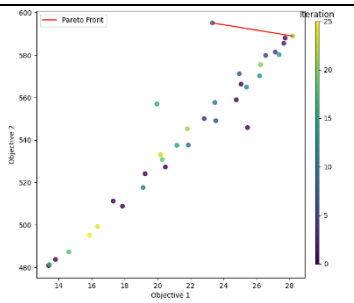

Figure 15: Proposed method for the Augmented dataset showing a) the starting point b) at 50% c) the full optimization

We then proceeded with an iterative approach, incrementally adding one data point at a time to expand the subset. For each new subset of data, we conducted another round of parameter optimization to maximize the objectives of interest. This iterative process enabled us to iteratively refine the parameter configuration, taking full advantage of the augmented dataset and its richer information content. The plot are shown in figure 15a to 15c with the optimization progress.

Table 8: Result for the augmented data

First Iteration	**50% of the Iteration**	**Pareto Front**
Hypervolume = 0.91	Hypervolume = 0.92	Hypervolume = 0.94
Proportional Hypervolume = 0.8	Proportional Hypervolume = 0.95	Proportional Hypervolume = 1
Generational Distance = 7.19	Generational Distance = 5.08	Generational Distance = 4.38
Inverted Generational Distance = 7.19	Inverted Generational Distance = 3.19	Inverted Generational Distance = 3.1

In our study, we observed hypervolume scores of 0.91, 0.92, and 0.94 at the initial, intermediate, and final stages of the optimization process, respectively. These results demonstrate a consistent improvement in the performance of the optimization methods as the process evolves. At the beginning, middle, and end of the optimization, the proportional hypervolume values were recorded as 0.96, 0.94, and 1, respectively. These scores indicate that the optimization methods

successfully enhanced the performance of the system, leading to increasingly superior outcomes throughout the process.

Our analysis revealed generational distance values of 7.19, 5.08, and 4.38, indicating a notable reduction in the average distance as the optimization progresses. These results signify the ability of the optimization methods to explore and converge toward solutions closer to the Pareto front. The inverted generational distance values observed were 7.19, 3.19, and 3.1, showcasing a substantial reduction in the distance as the optimization process advanced. These findings affirm the effectiveness of the optimization methods in identifying solutions that are closer to the true Pareto front.

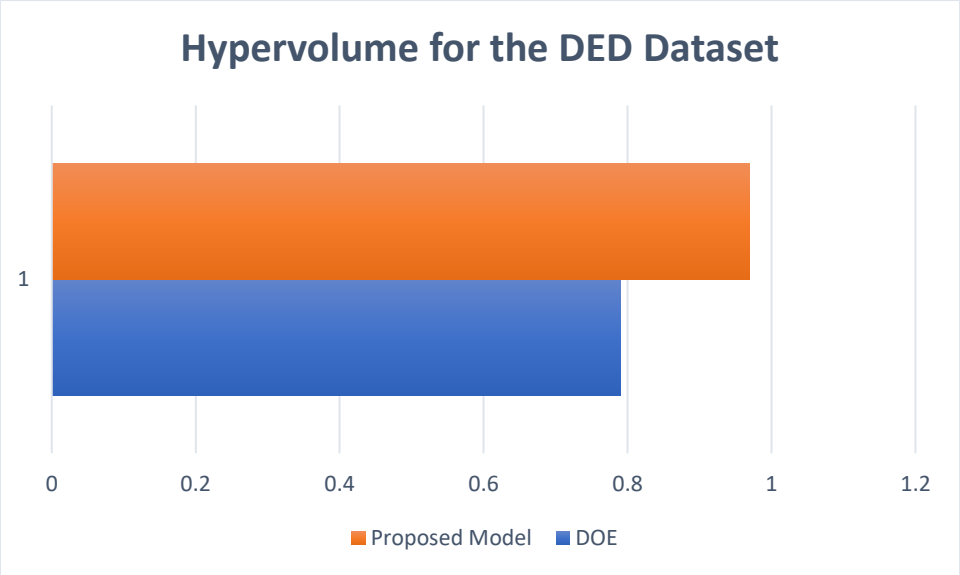

Figure 16: Hypervolume for the different approaches for the augmented data

The substantial difference in hypervolume values indicates that the proposed approach is a significant improvement over the traditional DOE method. Researchers and practitioners seeking to optimize their models and obtain superior results should consider implementing the proposed approach.

5.2. Analysis of the Prediction Model

In this section, we explore and analyze the comparative prediction results obtained from various machine learning (ML) models. These models are trained using three training datsets, i.e., training

data generated by the epsilon-greedy model, training data selected by DOE, and training data generated by random sampling. The ML-based prediction models utilized include Linear Regression, Random Forest Regression, and Lasso Regression. For comparison purposes, the same test data set has been utilized which is kept aside before the training phase. We also made sure that each training dataset contained the same number of data points.

5.2.1. Case-1: Material Design Space Data

Table 9 and 10 summarizes the prediction accuracy of Linear regression, Random forest regreeor, and Lasso regression using the epsilon-greedy model, random sampling, and the DOE models for the bulk and shear modulus respectively. As shown below in the table for both objectives, the epsilon-greedy model for prediction performs better than using the random sampling, DOE as it has a smaller RMSE which indicates that the predicted value is closer to the observed value. Also, it boasts having a higher accuracy which indicates that the model can have an explanation for most of the variability.

Table 9: Result summary comparing the approaches for the bulk modulus

Case	RMSE			R^2		
	Linear R	Random Forest	Lasso R	Linear R	Random Forest	Lasso R
Epsilon-greedy	31.90	25.86	31.93	0.44	0.63	0.44
Random sampling	32.61	31.95	32.59	0.50	0.52	0.50
DOE	39.85	42.70	50.88	0.14	0.02	0.39

We show the plot that shows the comparison between the result from the epsilon-greedy approach and the traditional prediction method approach. As it has been stated earlier, the higher the accuracy (R-square) the better our model is to predict the objective value correctly. Fig 17a shows that the epsilon-greedy approach works better in terms of accuracy than the DOE, and random sampling with the best result coming from the random forest regression with a 0.63 R-square value.

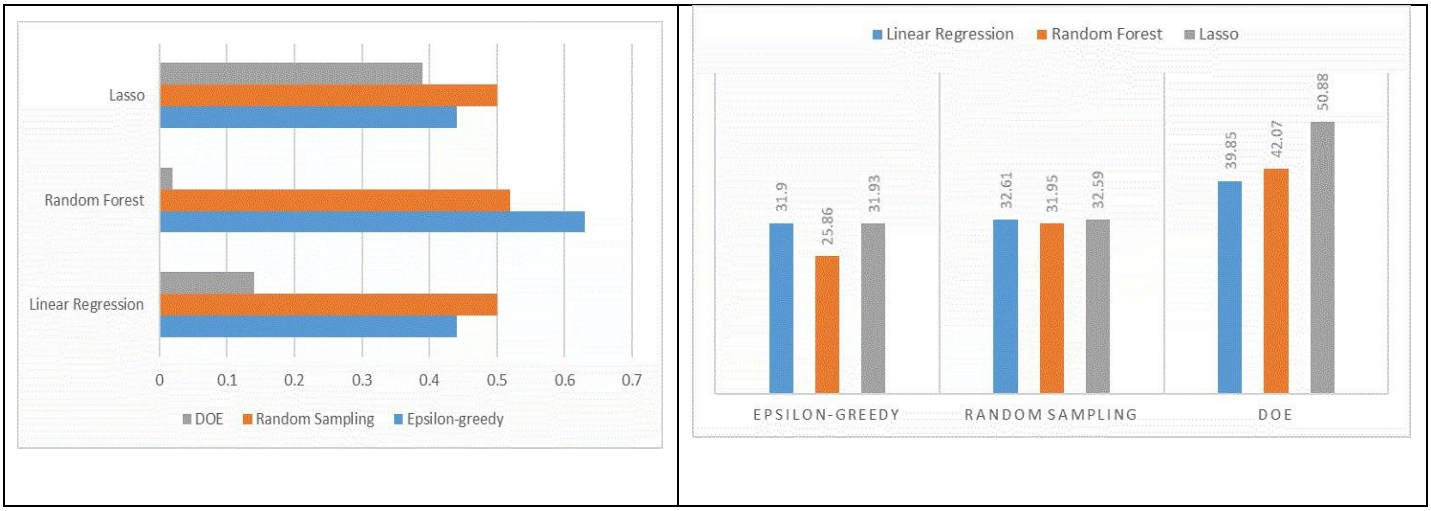

Figure 17: The comparison of the accuracy for different models for bulk modulus a) The accuracy b) the root mean square error

Fig 17b shows the error (RMSE), and this has also been noted that the lower the error the better the model is in achieving a better result. The epsilon-greedy approach works better than using the DOE or random sampling for the prediction.

Table 10: Result summary comparing different approaches for the shear modulus

Case	RMSE			R^2		
	Linear R	Random Forest	Lasso R	Linear R	Random Forest	Lasso R
Epsilon-greedy	16.15	13.93	16.13	0.67	0.76	0.67
Random Sampling	18.34	17.42	18.27	0.63	0.67	0.63
DOE	16.26	19.33	18.95	0.66	0.53	0.54

Figure 18 shows the comparison between the epsilon-greedy, random sampling and DOE approaches for the prediction of the bulk modulus. The Epsilon greedy approach has better accuracy and lower error compared to using the entire dataset.

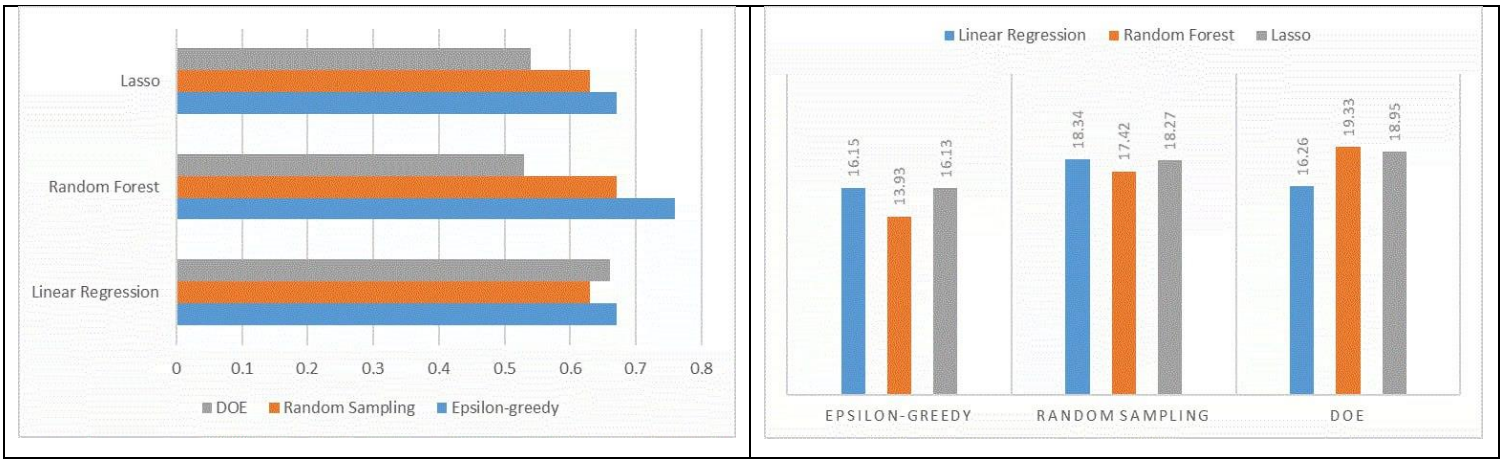

Figure 18: The comparison of the accuracy of the different models for shear modulus for a) accuracy b) root mean square error

5.2.2. Case-2: The DED Data

Tables 11 and 12 show the results of accuracy and Root Mean Squared Error (RMSE) for three different approaches: epsilon-greedy, Design of Experiments (DOE), and random sampling. These approaches were applied with various prediction models. The epsilon-greedy approach consistently outperformed the other two approaches.

The epsilon-greedy approach achieved higher accuracy and lower RMSE values than the DOE and random sampling methods. This was true for all of the prediction models that were tested.

The results indicate that the epsilon-greedy approach is a more effective way to generate accurate predictions and reduce errors. This suggests that the epsilon-greedy approach may be a better choice than the DOE or random sampling methods when working with different prediction models.

Table 11: Result summary comparing different approaches for the Elongation

Case	RMSE			R^2		
	Linear R	Random Forest	Lasso R	Linear R	Random Forest	Lasso R
Epsilon-greedy	2.19	2.43	2.01	0.81	0.76	0.85
Random sampling	2.0	3.3	2.39	0.85	0.59	0.78
DOE	3.1	3.15	3.01	0.65	0.64	0.67

Based on Figures 19 and 20, the epsilon-greedy approach exhibits superior performance in terms of r-square and RMSE compared to other approaches for the Elongation and Ultimate Tensile Strength (UTS) predictions. This trend holds for the majority of the prediction models, except for linear regression accuracy in the case of elongation.

For both elongation and UTS, the epsilon-greedy approach consistently outperforms other models in terms of accuracy and RMSE. This shows that the epsilon-greedy approach is generally more effective in providing accurate predictions and minimizing errors when compared to other models.

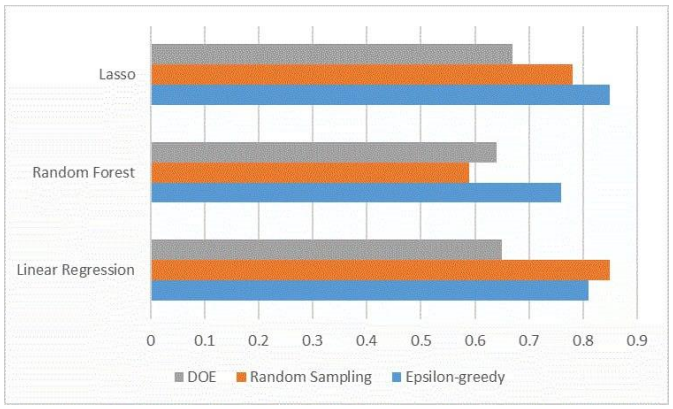

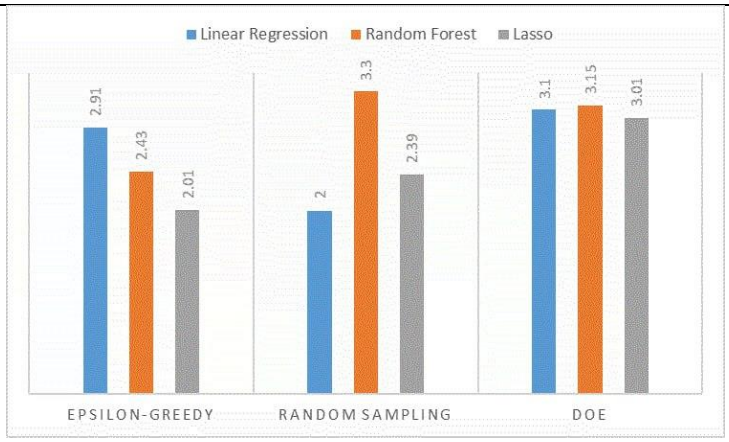

Figure 19: The comparison of the accuracy for different model for elongation showing a) The accuracy b) the root mean square error

However, it is worth noting that in the specific case of elongation and linear regression accuracy, the epsilon-greedy approach may not yield the highest accuracy. This implies that for elongation predictions with linear regression, alternative approaches or models may need to be considered to achieve optimal accuracy.

Table 12: Result summary comparing different approaches for the Ultimate Tensile Strength (UTS)

Case	RMSE			R^2		
	Linear R	Random Forest	Lasso R	Linear R	Random Forest	Lasso R
Epsilon-greedy	14.91	15.59	14.5	0.82	0.81	0.84
Random sampling	25.11	26.6	24.64	0.58	0.53	0.59
DOE	21.29	23.41	21.29	0.68	0.61	0.68

Overall, the findings from Figures 19 and 20 support the conclusion that the epsilon-greedy approach demonstrates better performance in terms of accuracy and RMSE compared to other models for most prediction scenarios, including UTS predictions.

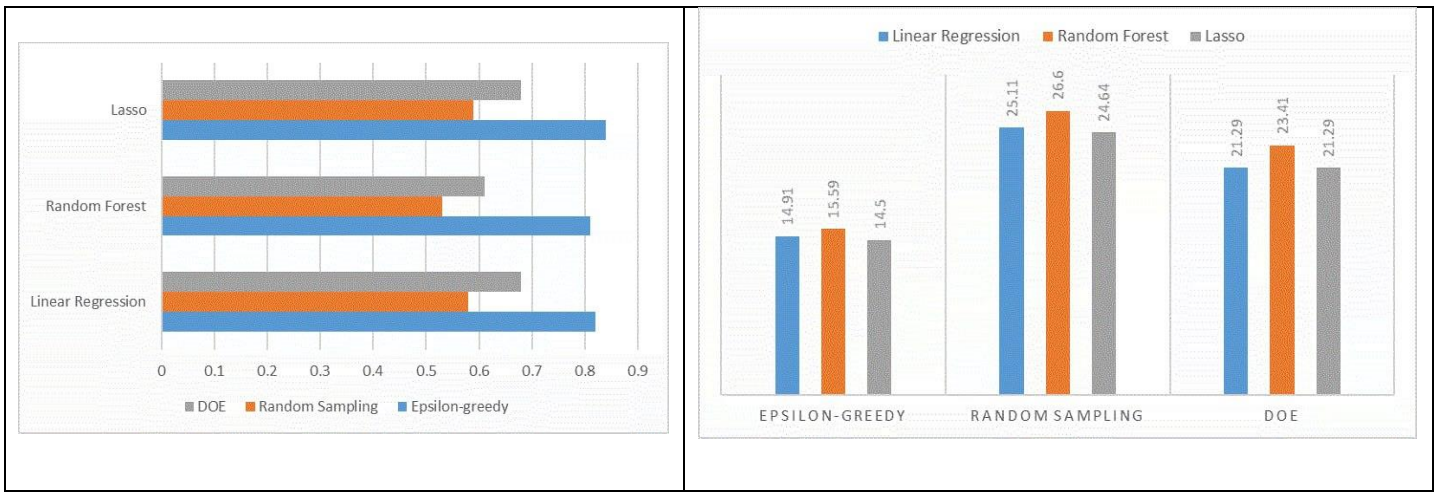

Figure 20: The comparison of the accuracy for different models for Ultimate Tensile Strength (UTS) showing a) The accuracy b) the root mean square error

6. Conclusion

This study aims to create a sequential decision-making framework to expedite manufacturing decisions. Depending on the underlying problem, both optimization and prediction frameworks are suggested. This research makes two crucial contributions. Firstly, a multi-objective Bayesian Optimization framework is developed to determine the optimal process parameters with minimal experimentation. A Gaussian Process-based surrogate model is utilized to represent the unknown design space or black-box function, while an acquisition function guides the framework in sequentially selecting experiments. The iterative model update process enables the framework to achieve the Pareto front in fewer iterations. Secondly, an epsilon-greedy prediction model is developed to balance exploration and exploitation, making the framework more prediction-friendly. The proposed frameworks optimize and predict faster and better compared to the alternatives and thus they are recommended to be adopted as real-time decision-making techniques in manufacturing.

This research has made important contributions to the field of manufacturing. However, it is important to acknowledge certain limitations. The quantity of the available data proved to be a constraint, potentially impacting the generalizability and scalability of the proposed frameworks.

As a result, it is recommended that future research focuses on modifying and adapting these frameworks to accommodate datasets with fewer data points, thus expanding their applicability in real-world scenarios.

Despite these limitations, the findings of this thesis provide valuable insights into the development of multi-objective Bayesian Optimization and epsilon-greedy sequential prediction frameworks in the context of manufacturing. The frameworks presented here offer promising avenues for optimizing processing conditions and approximating design spaces, leading to enhanced efficiency and performance within manufacturing settings. We hope that the outcomes of this research will inspire further investigation and encourage researchers to address the identified limitations, enabling the broader implementation and refinement of these frameworks. By doing so, the potential impact of these approaches on manufacturing processes can be maximized, ultimately contributing to the advancement of the field and facilitating more informed decision-making in industrial settings.

References

[1] Wang L. From intelligence science to intelligent manufacturing. Engineering 2019;5(4):615.

[2] Tao F, Cheng Y, Xu DL, Zhang L, Li BH. CCIoT-CMfg: cloud computing and Internet of Things-based cloud manufacturing service system. IEEE Trans Ind Inform 2014;10(2):14354.

[3] Baicun Wang a,b,c, Fei Tao d, Xudong Fang e,⇑, Chao Liu f, Yufei Liu c, Theodor Freiheit, Smart Manufacturing and Intelligent Manufacturing: A Comparative Review. 2020.

[4] Harding, J.A., Shahbaz, M., Srinivas, Kusiak, A., 2006. Data Mining in Manufacturing: A Review. Journal of Manufacturing Science and Engineering 128 (4), 969–976.

[5] S. Deshpande, L. T. Watson, and R. A. Canfield, "Pareto Front Approximation Using a Hybrid Approach," *Procedia Computer Science*, vol. 18, pp. 521–530, Jan. 2013, doi: 10.1016/j.procs.2013.05.216.

[6] G. Eichfelder, "An Adaptive Scalarization Method in Multiobjective Optimization," *SIAM J. Optim.*, vol. 19, no. 4, pp. 1694–1718, Jan. 2009, doi: 10.1137/060672029.

[7] B. Shahriari, K. Swersky, Z. Wang, R. P. Adams, and N. D. Freitas, "Taking the human out of the loop: A review of Bayesian optimization," *Proc IEEE*, vol. 104, no. 1, pp. 148–175, Jan. 2016, doi: 10.1109/JPROC.2015.2494218.

[8] J. Yang and Y. Liu, "Energy, time and material consumption modelling for fused deposition modelling process," *Procedia CIRP*, vol. 90, pp. 510–515, Jan. 2020, doi: 10.1016/j.procir.2020.02.130.

[9] J. Yang, Y. Chen, W. Huang, and Y. Li, "Survey on artificial intelligence for additive manufacturing," in *2017 23rd International Conference on Automation and Computing (ICAC)*, Sep. 2017, pp. 1–6. doi: 10.23919/IConAC.2017.8082053.

[10] B. Mueller, "Additive Manufacturing Technologies – Rapid Prototyping to Direct Digital Manufacturing," *Assembly Automation*, vol. 32, no. 2, Jan. 2012, doi: 10.1108/aa.2012.03332baa.010.

[11] K. Kellens, M. Baumers, T. G. Gutowski, W. Flanagan, R. Lifset, and J. R. Duflou, "Environmental Dimensions of Additive Manufacturing: Mapping Application Domains and Their Environmental Implications," *Wiley*, Aug. 2017, Accessed: Apr. 17, 2023. [Online]. Available: https://dspace.mit.edu/handle/1721.1/119453

[12] L. Bian, S. M. Thompson, and N. Shamsaei, “Mechanical Properties and Microstructural Features of Direct Laser-Deposited Ti-6Al-4V,” *JOM - Journal of the Minerals, Metals and Materials Society*, vol. 67, pp. 629–638, Mar. 2015, doi: 10.1007/s11837-015-1308-9.

[13] M. Dantin, W. Furr, and M. Priddy, *TOWARDS AN OPEN-SOURCE, PREPROCESSING FRAMEWORK FOR SIMULATING MATERIAL DEPOSITION FOR A DIRECTED ENERGY DEPOSITION PROCESS*. 2018.

[14] Y. Luo, Z. Ji, M. C. Leu, and R. Caudill, “Environmental performance analysis of solid freedom fabrication processes,” in *Proceedings of the 1999 IEEE International Symposium on Electronics and the Environment (Cat. No.99CH36357)*, May 1999, pp. 1–6. doi: 10.1109/ISEE.1999.765837.

[15] R. Sreenivasan and D. L. Bourell, “Sustainability Study in Selective Laser Sintering – An Energy Perspective”.

[16] J. K. Watson and K. M. B. Taminger, “A decision-support model for selecting additive manufacturing versus subtractive manufacturing based on energy consumption,” *Journal of Cleaner Production*, vol. 176, pp. 1316–1322, Mar. 2018, doi: 10.1016/j.jclepro.2015.12.009.

[17] S. Meteyer, X. Xu, N. Perry, and Y. F. Zhao, “Energy and Material Flow Analysis of Binder-jetting Additive Manufacturing Processes,” *Procedia CIRP*, vol. 15, pp. 19–25, Jan. 2014, doi: 10.1016/j.procir.2014.06.030.

[18] T. Peng and W. Sun, “Energy modelling for FDM 3D printing from a life cycle perspective,” *International Journal of Manufacturing Research*, vol. 12, pp. 83–98, Jan. 2017, doi: 10.1504/IJMR.2017.083651.

[19] J. Qin, Y. Liu, and R. Grosvenor, “Multi-source data analytics for AM energy consumption prediction,” *Advanced Engineering Informatics*, vol. 38, pp. 840–850, Oct. 2018, doi: 10.1016/j.aei.2018.10.008.

[20] O. Kwon *et al.*, “A deep neural network for classification of melt-pool images in metal additive manufacturing,” *J Intell Manuf*, vol. 31, no. 2, pp. 375–386, Feb. 2020, doi: 10.1007/s10845-018-1451-6.

[21] J. Zhang, P. Wang, and R. X. Gao, “Attention Mechanism-Incorporated Deep Learning for AM Part Quality Prediction,” *Procedia CIRP*, vol. 93, pp. 96–101, Jan. 2020, doi: 10.1016/j.procir.2020.04.051.

[22] Z. Zhang, Z. Liu, and D. Wu, “Prediction of melt pool temperature in directed energy deposition using machine learning,” *Additive Manufacturing*, vol. 37, p. 101692, Jan. 2021, doi: 10.1016/j.addma.2020.101692.

[23] F. Caiazzo and A. Caggiano, “Laser Direct Metal Deposition of 2024 Al Alloy: Trace Geometry Prediction via Machine Learning,” *Materials (Basel)*, vol. 11, no. 3, p. 444, Mar. 2018, doi: 10.3390/ma11030444.

[24] W. Rong-Ji, L. Xin-hua, W. Qing-ding, and W. Lingling, “Optimizing process parameters for selective laser sintering based on neural network and genetic algorithm,” *Int J Adv Manuf Technol*, vol. 42, no. 11, pp. 1035–1042, Jun. 2009, doi: 10.1007/s00170-008-1669-0.

[25] L. Jiang, H. Ye, C. Zhou, and S. Chen, “Parametric Topology Optimization Toward Rational Design and Efficient Prefabrication for Additive Manufacturing,” *Journal of Manufacturing Science and Engineering*, vol. 141, no. 4, Feb. 2019, doi: 10.1115/1.4042580.

[26] K. Aoyagi, H. Wang, H. Sudo, and A. Chiba, “Simple method to construct process maps for additive manufacturing using a support vector machine,” *Additive Manufacturing*, vol. 27, pp. 353–362, May 2019, doi: 10.1016/j.addma.2019.03.013.

[27] M. Mozaffar *et al.*, “Data-driven prediction of the high-dimensional thermal history in directed energy deposition processes via recurrent neural networks,” *Manufacturing Letters*, vol. 18, pp. 35–39, Oct. 2018, doi: 10.1016/j.mfglet.2018.10.002.

[28] Z. Li, Z. Zhang, J. Shi, and D. Wu, “Prediction of Surface Roughness in Extrusion-based Additive Manufacturing with Machine Learning,” *Robotics and Computer-Integrated Manufacturing*, vol. 57, Apr. 2019, doi: 10.1016/j.rcim.2019.01.004.

[29] J. Francis and L. Bian, “Deep Learning for Distortion Prediction in Laser-Based Additive Manufacturing using Big Data,” *Manufacturing Letters*, vol. 20, pp. 10–14, Apr. 2019, doi: 10.1016/j.mfglet.2019.02.001.

[30] G. Tapia, S. Khairallah, M. Matthews, W. E. King, and A. Elwany, “Gaussian process-based surrogate modeling framework for process planning in laser powder-bed fusion additive manufacturing of 316L stainless steel,” *Int J Adv Manuf Technol*, vol. 94, no. 9, pp. 3591–3603, Feb. 2018, doi: 10.1007/s00170-017-1045-z.

[31] M. Zhang *et al.*, “High cycle fatigue life prediction of laser additive manufactured stainless steel: A machine learning approach,” *International Journal of Fatigue*, vol. 128, p. 105194, Nov. 2019, doi: 10.1016/j.ijfatigue.2019.105194.

[32] M. Wu, V. Phoha, Y. Moon, and A. Belman, *Detecting Malicious Defects in 3D Printing Process Using Machine Learning and Image Classification*. 2016. doi: 10.1115/IMECE2016-67641.

[33] A. M. Aboutaleb, L. Bian, N. Shamsaei, S. M. Thompson, and P. K. Rao, "Multi-Objective Process Optimization of Additive Manufacturing: A Case Study on Geometry Accuracy Optimization".

[34] A. M. Aboutaleb, M. J. Mahtabi, M. A. Tschopp, and L. Bian, "Multi-objective accelerated process optimization of mechanical properties in laser-based additive manufacturing: Case study on Selective Laser Melting (SLM) Ti-6Al-4V," *Journal of Manufacturing Processes*, vol. 38, pp. 432–444, Feb. 2019, doi: 10.1016/j.jmapro.2018.12.040.

[35] N. Hertlein, K. Vemaganti, and S. Anand, "Bayesian Optimization of Energy-Absorbing Lattice Structures for Additive Manufacturing," *Volume 6: Design, Systems, and Complexity*, 2020, doi: 10.1115/imece2020-23377.

[36] C. Sharpe, C. C. Seepersad, S. Watts, and D. Tortorelli, "Design of Mechanical Metamaterials via Constrained Bayesian Optimization," in *Volume 2A: 44th Design Automation Conference*, Quebec City, Quebec, Canada: American Society of Mechanical Engineers, Aug. 2018, p. V02AT03A029. doi: 10.1115/DETC2018-85270.

[37] J. R. Deneault *et al.*, "Toward autonomous additive manufacturing: Bayesian optimization on a 3D printer," *MRS Bulletin*, vol. 46, no. 7, pp. 566–575, Jul. 2021, doi: 10.1557/s43577-021-00051-1.

[38] A. E. Gongora *et al.*, "A Bayesian experimental autonomous researcher for mechanical design," *Science Advances*, vol. 6, no. 15, p. eaaz1708, Apr. 2020, doi: 10.1126/sciadv.aaz1708.

[39] L. Cao, J. Li, J. Hu, H. Liu, Y. Wu, and Q. Zhou, "Optimization of surface roughness and dimensional accuracy in LPBF additive manufacturing," *Optics & Laser Technology*, vol. 142, p. 107246, Oct. 2021, doi: 10.1016/j.optlastec.2021.107246.

[40] M. Al Hazza, E. Adesta, M. Riza, and S. Suprianto, "Power Consumption Optimization in CNC Turning Process Using Multi Objective Genetic Algorithm," *Advanced Materials Research*, vol. 576, Oct. 2012, doi: 10.4028/www.scientific.net/AMR.576.95.

[41] A. Iqbal, H.-C. Zhang, L. Kong, and G. Hussain, “A rule-based system for trade-off among energy consumption, tool life, and productivity in machining process,” *Journal of Intelligent Manufacturing*, vol. 26, Nov. 2013, doi: 10.1007/s10845-013-0851-x.

[42] Y. Kumar and H. Singh, “Multi-response Optimization in Dry Turning Process Using Taguchi’s Approach and Utility Concept,” *Procedia Materials Science*, vol. 5, pp. 2142–2151, Jan. 2014, doi: 10.1016/j.mspro.2014.07.417.

[43] F. Kübler, J. Böhner, and R. Steinhilper, “Resource Efficiency Optimization of Manufacturing Processes Using Evolutionary Computation: A Turning Case,” *Procedia CIRP*, vol. 29, pp. 822–827, 2015, doi: 10.1016/j.procir.2015.02.208.

[44] M. Aria and C. Cuccurullo, “bibliometrix : An R-tool for comprehensive science mapping analysis,” *Journal of Informetrics*, vol. 11, no. 4, pp. 959–975, Nov. 2017, doi: 10.1016/j.joi.2017.08.007.

[45] A. Alvarado-Iniesta, L. Guillen-Anaya, L. Rodríguez-Picón, and R. Ñeco-Caberta, “Multi-objective optimization of an engine mount design by means of memetic genetic programming and a local exploration approach,” Journal of Intelligent Manufacturing, vol. 31, Jan. 2020, doi: 10.1007/s10845-018-1432-9.

[46] E. Natarajan, V. Kaviarasan, W. H. Lim, S. S. Tiang, S. Parasuraman, and S. Elango, “Non-dominated sorting modified teaching–learning-based optimization for multi-objective machining of polytetrafluoroethylene (PTFE),” *Journal of Intelligent Manufacturing*, vol. 31, no. 4, pp. 911–935, Apr. 2020, doi: 10.1007/s10845-019-01486-9.

[47] A. Törn and A. Zilinskas, *Global optimization*, vol. 350. Springer, 1989.

[48] D. R. Jones, M. Schonlau, and W. J. Welch, “Efficient Global Optimization of Expensive Black-Box Functions,” *Journal of Global Optimization*, vol. 13, no. 4, pp. 455–492, Dec. 1998, doi: 10.1023/A:1008306431147.

[49] S. Greenhill, S. Rana, S. Gupta, P. Vellanki, and S. Venkatesh, “Bayesian Optimization for Adaptive Experimental Design: A Review,” *IEEE Access*, vol. 8, pp. 13937–13948, 2020, doi: 10.1109/ACCESS.2020.2966228.

[50] A. Mathern *et al.*, “Multi-objective constrained Bayesian optimization for structural design,” *Struct Multidisc Optim*, vol. 63, no. 2, pp. 689–701, Feb. 2021, doi: 10.1007/s00158-020-02720-2.

[51] A. Biswas, A. N. Morozovska, M. Ziatdinov, E. A. Eliseev, and S. V. Kalinin, "Multi-objective Bayesian optimization of ferroelectric materials with interfacial control for memory and energy storage applications," *Journal of Applied Physics*, vol. 130, no. 20, p. 204102, Nov. 2021, doi: 10.1063/5.0068903.

[52] J. Knowles, "ParEGO: A Hybrid Algorithm With On-Line Landscape Approximation for Expension Multiobjective Optimization Problems," *Evolutionary Computation, IEEE Transactions on*, vol. 10, pp. 50–66, Mar. 2006, doi: 10.1109/TEVC.2005.851274.

[53] T. Simpson, F. Mistree, J. Korte, and T. Mauery, "Comparison of response surface and kriging models for multidisciplinary design optimization," in *7th AIAA/USAF/NASA/ISSMO Symposium on Multidisciplinary Analysis and Optimization*, in Multidisciplinary Analysis Optimization Conferences. American Institute of Aeronautics and Astronautics, 1998. doi: 10.2514/6.1998-4755.

[54] J. Davins, S. Moussaoui, F. Plestan, and G. Gil, "ParEGO Extensions for Multi-objective Optimization of Expensive Evaluation Function," *Journal of Global Optimization*, vol. 67, Jan. 2017, doi: 10.1007/s10898-016-0419-3.

[55] A. M. Aboutaleb, L. Bian, N. Shamsaei, S. Thompson, and P. Rao, *Multi-objective Process Optimization of Additive Manufacturing: A Case Study on Geometry Accuracy Optimization*. 2016.

[56] Wang L. From intelligence science to intelligent manufacturing. Engineering 2019;5(4):615.

[57] Tao F, Cheng Y, Xu DL, Zhang L, Li BH. CCIoT-CMfg: cloud computing and Internet of Things-based cloud manufacturing service system. IEEE Trans Ind Inform 2014;10(2):14354.

[58] Baicun Wang a,b,c, Fei Tao d, Xudong Fang e,⇑, Chao Liu f, Yufei Liu c, Theodor Freiheit, Smart Manufacturing and Intelligent Manufacturing: A Comparative Review. 2020.

[59] Barsoum, M. W. (2013). Max phases properties of machinable ternary carbides and nitrides. Wiley.

[60] Barsoum, M. W. (2000). The MN+1AXN phases: A new class of solids. Progress in Solid State Chemistry, 28(1-4), 201–281. https://doi.org/10.1016/s0079-6786(00)00006-6

[61] Barsoum, M. W., & Radovic, M. (2011). Elastic and mechanical properties of the Max Phases. Annual Review

[62] Amini, S., & Barsoum, M. W. (2010). On the effect of texture on the mechanical and damping properties of nanocrystalline MG-matrix composites reinforced with Max Phases. Materials Science and Engineering: A, 527(16-17), 3707–3718. https://doi.org/10.1016/j.msea.2010.01.073

[63] Aryal, S., Sakidja, R., Barsoum, M. W., & Ching, W.-Y. (2014). A genomic approach to the stability, elastic, and electronic properties of the Max Phases. Physica Status Solidi (b), 251(8), 1480–1497. https://doi.org/10.1002/pssb.201451226

[64] Talapatra, A., Boluki, S., Duong, T., Qian, X., Dougherty, E., & Arróyave, R. (2018). Autonomous Efficient Experiment Design for Materials Discovery with bayesian model averaging. Physical Review Materials, 2(11). https://doi.org/10.1103/physrevmaterials.2.113803